

Development of Test Methods for Evaluation of Bending Stiffness and Compressive Modulus of Braided Composite Lattice Structures

by

Sanyam Jeevan Shirgaonkar

A thesis submitted to the Graduate Faculty of
Auburn University
In partial fulfillment of the
requirements for the Degree of
Master of Science

Auburn, Alabama
May 9, 2015

Keywords: open architecture composite structures (O-ACS), test methods,
bending stiffness, compressive modulus

Copyright 2015 by Sanyam Jeevan Shirgaonkar

Approved by

David Beale, Chair, Professor of Mechanical Engineering
Royall Broughton, Jr., Co-chair, Professor Emeritus of Polymer and Fiber Engineering
Sabit Adanur, Professor of Polymer and Fiber Engineering
Winfred Foster, Professor of Aerospace Engineering

Abstract

Open Architecture Composite Structures (O-ACS) have been recently developed and are known for their high modulus per unit weight. They are truss structures preformed on a mandrel shaped as a cylindrical, elliptical or polygonal cross section tube. It is very critical to accurately measure the mechanical properties of these structures in order to evaluate and optimize them. This work focuses on development of test methods suitable and appropriate for testing O-ACS to accurately and precisely measure the bending stiffness and axial stiffness under compression. The current research includes testing the O-ACS with standard three point bending test and further improving the test method to be more accurate for O-ACS specific testing, by using collars to reduce the localized deflection. A novel test method for measuring bending stiffness of O-ACS has then been introduced with an intention to provide more accurate and consistent results. In this test method the specimen is potted in epoxy and steel extensions are attached on both ends. Forces are then applied on these extensions to apply a pure moment to the specimen, thus eliminating deflection due to shear as well as contact stresses. A test method for accurately measuring the compressive stiffness and compressive modulus is developed in this research. Different configurations of O-ACS (Varying the number of axial yarns and braid angle) are tested for a comparative study of their compressive stiffness and moduli. Custom test fixtures built for performing these test methods have also been described in detail as a part of this study. The effect of molding Expanded Polypropylene (EPP) inside the O-ACS on the bending stiffness of O-ACS has also been studied.

Acknowledgements

I would like to thank my parents for encouraging me to pursue higher education and for their enduring love and teachings. It is their teachings that make the good in me. I would like to express deep gratitude to my brother Aniket and my sister in law Gauri for their nurturing love and moral support. I thank them for always being there for me and never letting me feel away from home. It is by following Aniket's footsteps that I chose Auburn's Mechanical Engineering Program.

I am grateful to Dr. Beale to have accepted me as his student and financially supporting me in my graduate program. He has been a constant source of knowledge and advice. I thank him for being very patient and forgiving throughout this journey. I have been educated in various aspects by him.

I must thank Dr. Broughton for his invaluable guidance and direction in my research. I have learnt from him to find simple solutions to seemingly difficult problems. I would also like to thank Dr. Adanur and Dr. Foster for their beneficial inputs and suggestions in the weekly research meetings and to have accepted to be on my Masters committee. Special thanks go to Dr. Suhling, the department chair, for supporting me financially in the first year of my program and for being very helpful and co-operative.

I cannot thank Austin Gurley enough for all the knowledge and insight in mechanical engineering that he has provided me with. He has been extremely helpful and has contributed

significantly to this research at each step. I admire his dedication to every task he does and his attitude towards problems faced while working. I am deeply inspired by him and strive to attain his quality of working.

I would like to thank Dr. Banscomb for sharing his work, passing over his knowledge and for his consistent willingness to help in research. I must thank Nakul Kothari, Shane Furlong, Yang Shen and Caleb Peterson, for all the help and information they have provided for this research. It was a pleasure working with them. I also express my gratitude to Amith Jain and Bala Murugan Sundaram for the brainstorming sessions on my research, their valuable suggestions as well as for helping me in my coursework.

I take this opportunity to thank Jordan French for understanding the importance of finishing my thesis and taking over my Formula SAE responsibilities for me to focus on my thesis. I have been blessed with caring roommates Rishi Kamat and Akash Shettannavar who understood the work load I had and always helped without a complaint and constantly supported me.

I must thank Sharwari Patil for persistently pushing me to work harder and reminding me that my thesis is my first priority. Lastly, I thank all my dear friends and family in India for their love, support and understanding my lack of contact when I needed time for completing my thesis.

Table of Contents

Abstract.....	ii
Acknowledgements.....	iii
List of Illustrations.....	vii
Introduction	1
Summary	1
Overview of O-ACS manufacturing	2
Overview of yarn manufacturing	3
Important mechanical properties of O-ACS.....	4
Bending Stiffness.....	5
Introduction	5
ASTM Standards.....	5
Three Point bending test	13
Modified Three Point Bending Test	20
Validation	21
Testing.....	28
Conclusions	31
Pure moment test (Modified Four Point Bending Test)	32
Validation	36
Testing.....	42
Conclusion.....	45
Compressive Stiffness and Modulus.....	46
Introduction	46
ASTM Standards.....	46
Test setup.....	50
Validation.....	52
Testing.....	55

Results.....	58
Effect of Expanded poly propylene on bending stiffness of O-ACS	62
Introduction	62
O-ACS with EPP	63
Testing.....	67
Conclusion.....	71
References	73

List of Illustrations

Figure 1 O-ACS during manufacturing [2].....	2
Figure 2 Manufacturing of Braid-able composite yarn [1]	3
Figure 3 Standard Three Point Bending Test [3]	6
Figure 4 Loading noses spaced apart, 1/3rd of the support span [4].....	7
Figure 5 Loading noses spaced apart, half of the support span [4].....	7
Figure 6 Loading noses and supports [4]	8
Figure 7 Cross section of test specimen [5]	9
Figure 8 Use of anvils for supporting cylindrical specimen [5].....	10
Figure 9 Research path followed	12
Figure 10 Isometric view of the 3D model of three point bending fixture	13
Figure 11 Drawings showing dimensions used in building the 3 point bending fixture.....	14
Figure 12 Specimen Illustrations and specifications.....	15
Figure 13 Three Point bending test on O-ACS tube	16
Figure 14 Force - Deflection curves measured at the top and the bottom of the O-ACS	17
Figure 15 Three Point Bending Test on Aluminum tube	18
Figure 16 Force - Deflection Curves measured at the top and the bottom of the Aluminum tube	19
Figure 17 The Front view, Side view and the Isometric view of the Collar	20
Figure 18 Aluminum tube while testing in three point bending with collars.....	21
Figure 19 Force-Deflection Curves on Aluminum tube with and without collars.....	22
Figure 20 Force - Deflection curves of aluminum tube tested in three point bending with collars	23

Figure 21 Variation in Bending Stiffness EI with changing span length.....	24
Figure 22 Comparison between measured deflection and analytical deflection and contribution of the correction factors required to eliminate to this difference	27
Figure 23 Performing modified Three point bending test on the O-ACS.....	28
Figure 24 Force - Deflection curves from the modified three point bend test performed on O-ACS with fro different span lengths (600mm – 1200mm)	29
Figure 25 Variation in bending stiffness measured using modified three point bending test with changing span length	30
Figure 26 3D Model of the Assembled Pure Moment Fixture with an illustration of a specimen	32
Figure 27 Drawings and specifications of the nipples and couplings used for potting.....	33
Figure 28 Epoxy resin and hardener used for potting	34
Figure 29 Stepwise procedure for potting the specimen [2]	35
Figure 30 Potting the ends of the Aluminum tube Figure 31 Potting the ends of the O-ACS.....	36
Figure 32 The Aluminum tube being tested in pure moment test.....	37
Figure 33 Measuring the Stiffness of the fixture	38
Figure 34 Geometric constructions to help in calculating the bending stiffness (EI)	39
Figure 35 Comparison of bending stiffness values for aluminum tube obtained from the Pure Moment Test, from the Modified Three Point Bend test and from the analytical solution.....	41
Figure 36 Testing of O-ACS using Pure Moment Test.....	42
Figure 37 Comparison between bending stiffness values obtained from Pure Moment Test and Modified 3 Point Bending Test.....	43
Figure 38 Adjustable bearing blocks [10] Figure 39 Spherically seated bearing blocks [10]	47
Figure 40 Example of a Compression testing apparatus [10]	47

Figure 41 Sub press for compression tests	Figure 42 Compression tool	48
Figure 43 3D model of the compression fixture		50
Figure 44 Compression Test fixture.....		51
Figure 45 Aluminum tube with potted ends being tested in the compression fixture.....		52
Figure 46 Force deflection curve from the compression test performed on the aluminum tube		53
Figure 47 Comparison between the experimentally obtained compressive modulus and the analytical solution.....		54
Figure 48 Testing the O-ACS in the compression fixture.....		56
Figure 49 Force Deflection Curves of various O-ACS tested.....		57
Figure 50 Comparison between axial stiffness of various configurations of O-ACS.....		58
Figure 51 Comparison between axial specific stiffness of various configurations of O-ACS.....		59
Figure 52 Comparison between compressive modulus of various configurations of O-ACS		60
Figure 53 Polypropylene pellets	Figure 54 Expanded polypropylene beads	62
Figure 55 1 inch O_ACS held in supports to be placed in the mold of an EPP molding machine		64
Figure 56 1 inch O-ACS held in supports placed in the mold of an EPP molding machine.....		64
Figure 57 EPP molding machine		65
Figure 58 1 inch diameter O-ACS tube (1.549 gm/cm).....		65
Figure 59 1 inch diameter O-ACS tube with EPP molded inside it (1.736 gm/cm)		66
Figure 60 1 inch O-ACS being tested in 3 point bending		67
<i>Figure 61 1 inch O-ACS with EPP molded in it being tested in 3 point bending</i>		<i>68</i>
Figure 62 Force - Deflection Curves from 3 point bending test performed on O-ACS with and without EPP molded inside		68
Figure 63 1 inch O-ACS being tested in modified 3 point bending.....		69

Figure 64 1 inch O-ACS with EPP molded in it being tested in modified 3 point bending 70

Figure 65 Force - Deflection Curves from 3 point bending test performed on O-ACS with and without
EPP molded inside 71

List of abbreviations

O-ACS	Open Architecture Composite Structures
EPP	Expanded polypropylene

Introduction

Summary

The world today is moving rapidly towards light weight solutions in all areas of engineering. From aircraft to bicycles all the industries have started using carbon fiber, fiber glass, Kevlar® fiber reinforced polymer composites for their known high strength to weight and stiffness to weight ratios. Another way of obtaining higher strength or stiffness at lower weight is by making use of geometry, for example by using a truss structure rather than a solid one. With this objective of gaining high stiffness to weight ratio Dr. Branscomb researched and successfully developed truss preforms in flat, polygon or cylindrical form using braiding technology to arrange the yarns.¹ Much of this work can be found in the work of David Branscomb (Branscomb, Minimal Weight Composites Utilizing Advanced Manufacturing Techniques, 2012). In this work minimal weight composite structures were designed, manufactured and tested. It is very important to accurately measure the various mechanical properties of these Open Architecture Composite Structures (O-ACS) in order to evaluate and optimize them. In the current research various standard test methods for measuring bending stiffness and compressive stiffness including ASTM D790, ASTM D6272, ASTM D4476, ASTM D7249, ASTM D7250, ASTM E9, ASTM D695 are investigated for their applicability in testing O-ACS. New test methods, taking the three point bending test, four point bending test and compression test as references, are developed to suit the geometry of the O-ACS to accurately and precisely measure the bending stiffness and the compressive stiffness. It is important to note that none of the O-ACS geometries used in this research were optimal for the

specific loading conditions and were made for the sole purpose of developing and validating the test methods and apparatuses.

Overview of O-ACS manufacturing

The O-ACS are manufactured using a conventional braiding machine. Appropriate carriers on the machine are loaded to get the specific geometry combined with the axial yarns that run along the length of the structure and are braided over a mandrel, typically made of aluminum or any other stiff material, which defines the major dimensions of the structure. Figure 1² shows an O-ACS tube being manufactured.



Figure 1 O-ACS during manufacturing [2]

Overview of yarn manufacturing

The yarn used in manufacturing O-ACS is made up of a core which has a high stiffness to weight ratio and is covered by braiding a jacket of textile fibers on it. The core is usually made of resin-impregnated carbon fiber tows which give much of the stiffness and strength to the yarn and therefore to the structure. Resin impregnated carbon fiber tows by themselves are sticky and not braidable. The textile fibers braided around the jacket increase the braidability of the yarn; they do not contribute towards strength or stiffness much. The yarn is braided on a Maypole braiding machine as shown in Figure 2 [1] where the yarn is pulled horizontally at a constant speed. A mechanism consisting of pulleys and sensors (not shown in the picture) to maintain constant tension in the yarn during braiding.

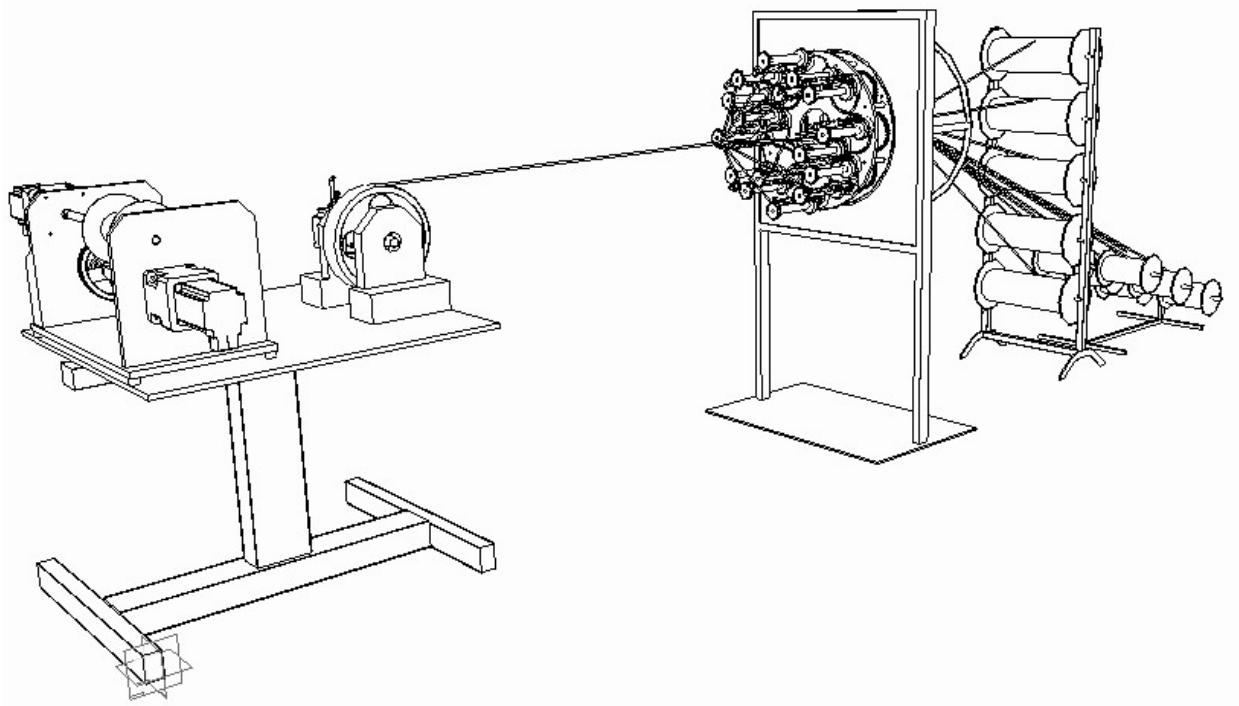


Figure 2 Manufacturing of Braid-able composite yarn [1]

Important mechanical properties of O-ACS

We intend to use the O-ACS as structural member which would act as a beam, a column or a load bearing member in a truss. The O-ACS would therefore have to bear forces applied to them in tension, compression and bending. Thus the most critical mechanical properties of the O-ACS are their ability to resist deflection caused by bending and axial loads, which are termed as bending stiffness and axial stiffness. Along with the stiffness it is equally important to evaluate the modulus which is the ratio of the stress and the strain and the strength which is the breaking force. The end goal of this research is to develop test methods that can accurately and precisely measure the stiffness and modulus of the O-ACS in bending and in compression.

Bending Stiffness

Introduction

Bending stiffness is one of the most important properties of a structural element. As our purpose is to use the O-ACS as structural elements, being able to measure their ability to resist bending is significant. Bending stiffness describes the degree to which a beam resists deflection in bending.

ASTM Standards

There are various ASTM Standard tests available for measuring bending stiffness and bending strength of different materials. Following is a brief description of the available tests:

D790, D7249, D7250, D4476, D6272

ASTM D790 [³] - Flexural Properties of Unreinforced and Reinforced Plastics (THREE POINT BENDING TEST)

This is a standard three point bend test, in which the specimen to be tested is a simply supported beam loaded at three points. The three points of loading include two supports and a loading nose. Several type of specimens, including reinforced and unreinforced plastics, high modulus composites and electrical insulating materials can be tested to evaluate their flexural properties. The test specimens are in the form of rectangular bars which rests upon two supports and is loaded midway between the supports using the loading nose. The span length to depth ratio (L/D) is recommended to be 16:1 but larger ratios can be used if necessary for certain materials.

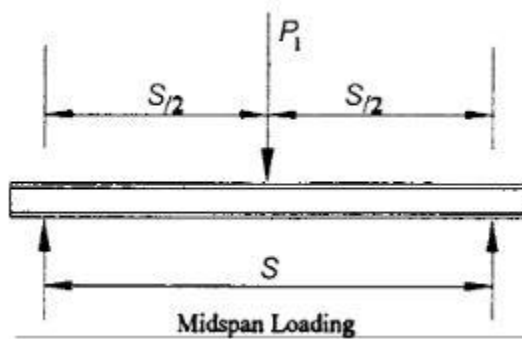


Figure 3 Standard Three Point Bending Test [3]

As the test method requires rectangular specimens it isn't very suitable for testing O-ACS but we can still consider using other details advised by the test method such as the Span-to-depth ratio (considering the diameter of the tube as depth), support nose radius and loading nose radius.

All the three points in this test method, the loading point and the two supports are point loads, which do not work very well on open, cylindrical structures (O-ACS) as the single joint or the small section of a single yarn on which the load is applied deforms significantly giving a false and lower stiffness due to this localized deflection. Deflection due to shear is significant which leads to inaccurate determination of bending stiffness of O-ACS.

ASTM D6272⁴ - Standard Test Method for Flexural Properties of Unreinforced and Reinforced Plastics (FOUR POINT BENDING TEST) [4]

This is a standard four point bend test which employs a four point loading system to a simply supported beam. The basic difference between ASTM D790 and ASTM D6272 is that there are two loading noses in the later as opposed to just one in the former. The application of load at four points in such a manner results in a region in between the loading noses where the maximum axial

fiber stress is uniformly distributed and observes maximum bending moment. Several type of specimens, including reinforced and unreinforced plastics, high modulus composites and electrical insulating materials can be tested to evaluate their flexural properties. The test specimens are in the form of rectangular bars rests upon two supports and each of the loading noses is at an equal distance from the adjacent support. The distance between the loading noses (the load span) is either one third or one half of the support span (Figure 4 and Figure 5). The span length to depth ratio (L/D) is recommended to be 16:1 but larger ratios can be used if necessary for certain materials or for any other specific reason.

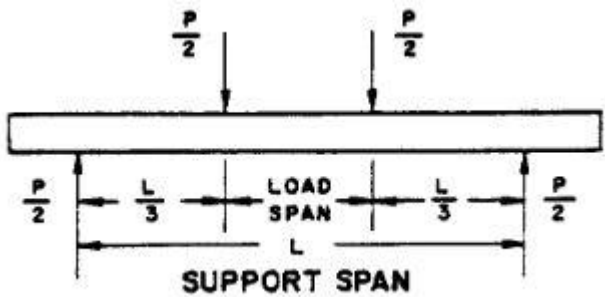


Figure 4 Loading noses spaced apart, 1/3rd of the support span [4]

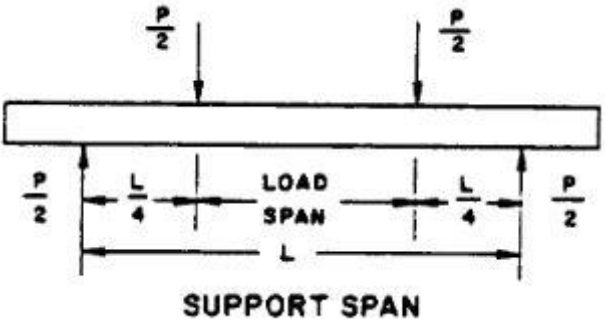


Figure 5 Loading noses spaced apart, half of the support span [4]

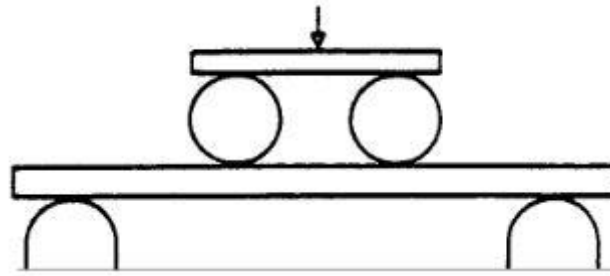


Figure 6 Loading noses and supports [4]

The effect due to shear can be reduced significantly by using this test method but the problem of localized crushing of individual yarns still exists. Furthermore the standard recommends the usage of rectangular bars which is not possible in case of O-ACS.

If the recommended span length for a given depth of specimen was to be used for the varying sizes of O-ACS, the fixture would have to be adjustable to a very long length of more than 6 feet. This would also mean that for carrying out an optimization study or any other type of study which involves rigorous testing of O-ACS, long lengths of O-ACS would have to be made, as specimens, which would require enormous amount of time, human labor and material.

ASTM D4476⁵ - Standard Test Method for Flexural Properties of Fiber Reinforced Pultruded Plastic Rods

This test method is similar to ASTM D790 (three point bending test) and is applicable to fiber-reinforced pultruded plastic rods. The specimen is a rod with a semicircular cross section, cut from lengths of pultruded rods to be tested (Figure 7). The diameter of the rod to be tested is ½ inch or greater.

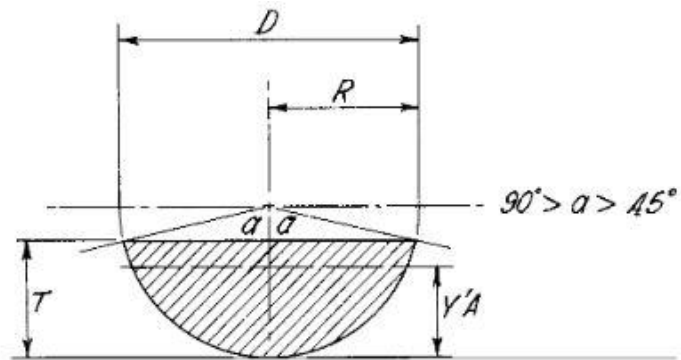


Figure 7 Cross section of test specimen [5]

The supports, used in this test method, consist of anvils to support the round sections (See Figure 8). The specimen rests on two such anvils and is loaded by means of a loading nose midway between the supports. “The use of the semicircular cross section eliminates premature compression shear that has been noted in three-point flexure tests on full-round rods. The loading nose has cylindrical surfaces in order to avoid excessive indentation or failure due to stress concentration directly under the loading nose” [5].

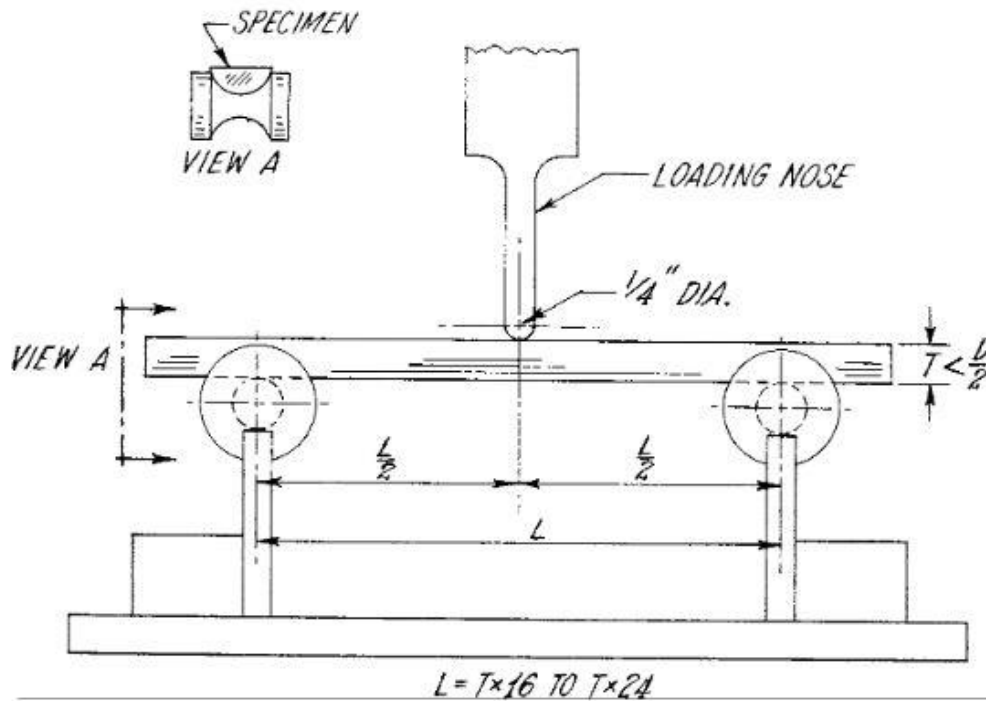


Figure 8 Use of anvils for supporting cylindrical specimen [5]

This test method cannot be used exactly the way it is described, for the obvious reason that if the O-ACS are cut into half to make a semicircular tube, they lose their mechanical properties, but the shape of the supports is very interesting and could be useful for testing O-ACS. The use of these anvils might reduce the loading on individual yarns and distribute the load over other surrounding yarns, reducing the localized deflection.

ASTM D7250⁶ - Standard Practice for Determining Sandwich Beam Flexural and Shear Stiffness

“This practice covers determination of the flexural and transverse shear stiffness properties of flat sandwich constructions subjected to flexure in such a manner that the applied moments produce curvature of the sandwich facing planes.”

The above test standard relates to sandwich structures and do not have much relevance to O-ACS tube testing but were still reviewed as they are related to flexural properties of composite structures.

ASTM D7249⁷ - Standard Test Method for Facing Properties of Sandwich Constructions by Long Beam Flexure

This test method covers determination of facing properties of flat sandwich constructions subjected to flexure in such a manner that the applied moments produce curvature of the sandwich facing planes and result in compressive and tensile forces in the facings.

The above test standard relates to sandwich structures and do not have much relevance to O-ACS tube testing but were still reviewed as they are related to flexural properties of composite structures.

All the above test methods are used as references while forming new test methods for testing O-ACS. For all the test methods that have been used in the following sections, thin walled aluminum tubes were tested for validation. There are several advantages of using thin walled aluminum tubes for validation such as:

1. Localized crushing is observed in a thin walled aluminum tubes like in O-ACS
2. The inertia of a thin walled aluminum tube is low similar to O-ACS
3. Shear factor (effect due to shear deformation) has a considerable effect on the bending stiffness
4. Properties of Aluminum are known and thus help in validation

The path of research followed for establishing test methods and standards for O-ACS is described in the flow chart below:

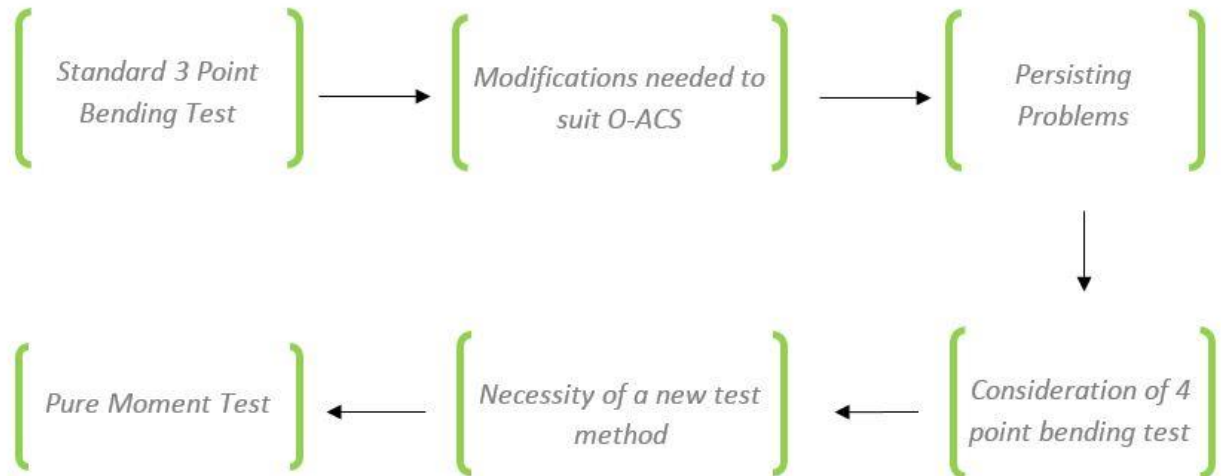


Figure 9 Research path followed

Three Point bending test

Three point bending test is a widely accepted standard test for measuring bending stiffness; it was therefore used as a starting point of this section of research. A three point bending test rig was built by using the ASTM D790 standard test as a reference. Necessity was felt for the test rig to have an adjustable span, as the diameters of O-ACS tube specimens would be varying; also the ideal length to diameter ratio to be used for O-ACS was not pre-determined. The CAD model and drawings describing the fixture are shown in the Figure 10 and Figure 11 respectively.

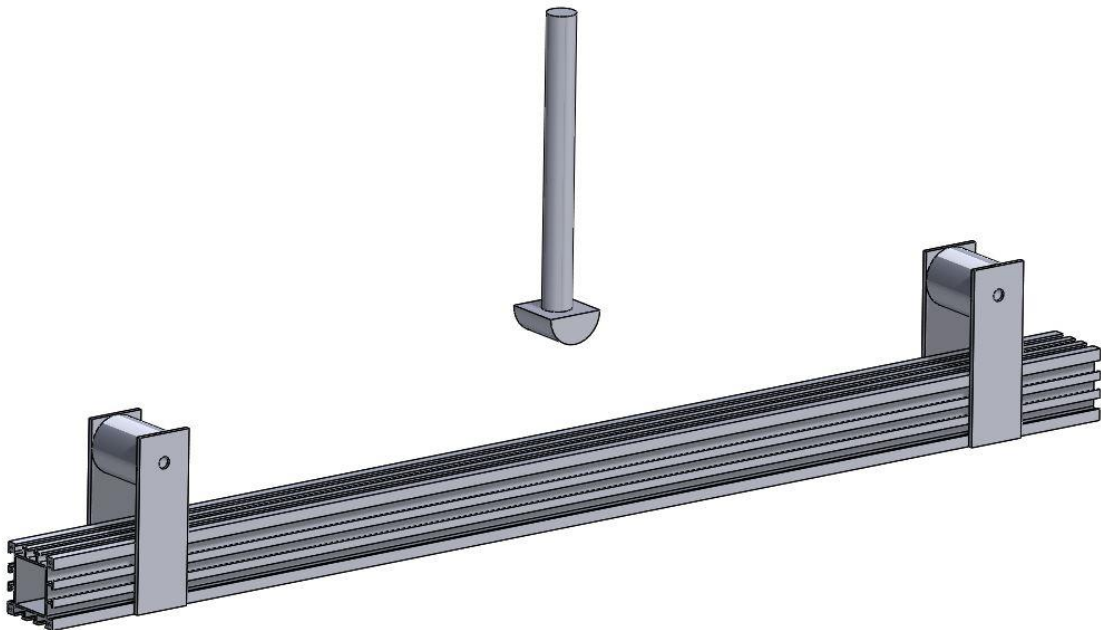


Figure 10 Isometric view of the 3D model of three point bending fixture

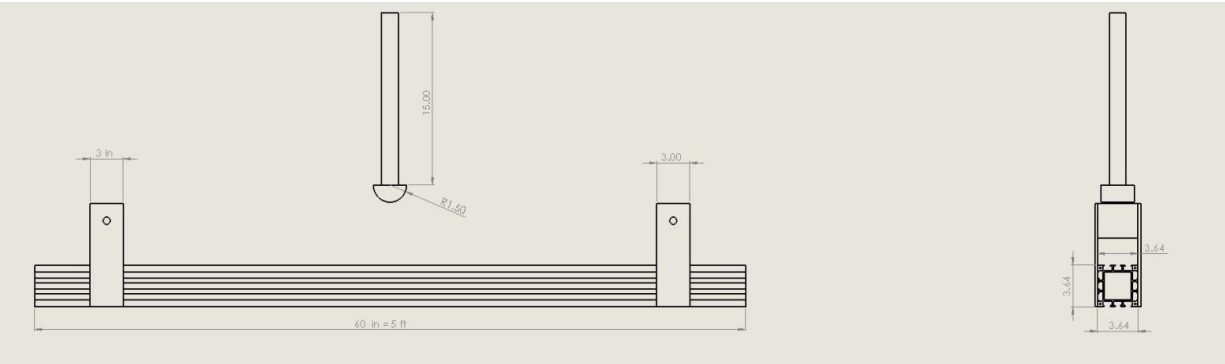
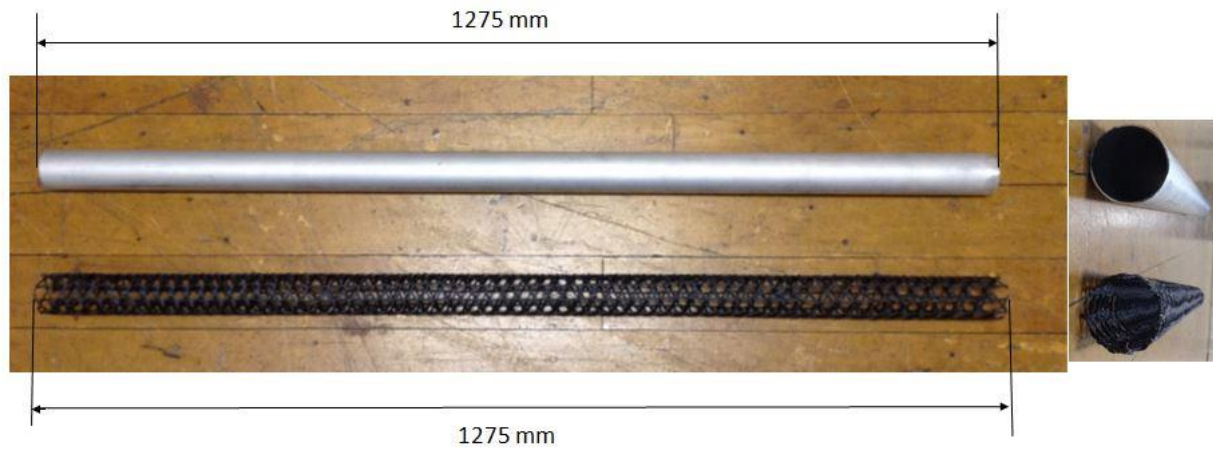


Figure 11 Drawings showing dimensions used in building the 3 point bending fixture

The ASTM D790 standard recommends the support diameter to be between 3.2 mm to 3 times the specimen depth and the nose radius to be between 3.2 mm to 4 times the specimen depth. These requirements for nose and support diameters were well within the range. The fixture was made to be adjustable from 3 inches to 60 inches (5 feet) with supports free to rotate about their own axes so that it does not resist the bending. An Aluminum tube and an Open structure with similar dimensions were used as specimens for performing the tests. Figure 12 shows the visuals of the specimens and their specifications.



	Elastic Modulus (E)	Outside Diameter	Wall Thickness	Inertia (I) (mm ⁴)	Bending Stiffness (EI) (10 ⁶ Nmm ²)	Weight/unit length (gm/mm)
Aluminum	69 GPa	2 in	.035in	43419.8	2996	0.380
Open Structure	-	2 in	0.2in	Varies with orientation	To be found Experimentally	0.172

Figure 12 Specimen Illustrations and specifications

The O-ACS tube was made of 8 axial yarns equally spaced around the circumference and 8 helical yarns (4 warps and 4 wefts). Each yarn was made of a core and a jacket. The core of the yarn consisted of 48K carbon fiber reinforced polymer matrix pre-impregnated tows. The jacket was made up of axial and helical tows. 8 axial fibers were used, all of which were 3K T300 carbon fiber reinforced polymer matrix pre-impregnated tows. Eight helical yarns were used in the jacket, 4 going clockwise and the other 4 going counter clockwise, each of these were 500 denier nylon.

Localized deflection at the point of loading was suspected while testing and therefore the deflections both at the top and the bottom of the O-ACS were recorded as shown in the Figure 13

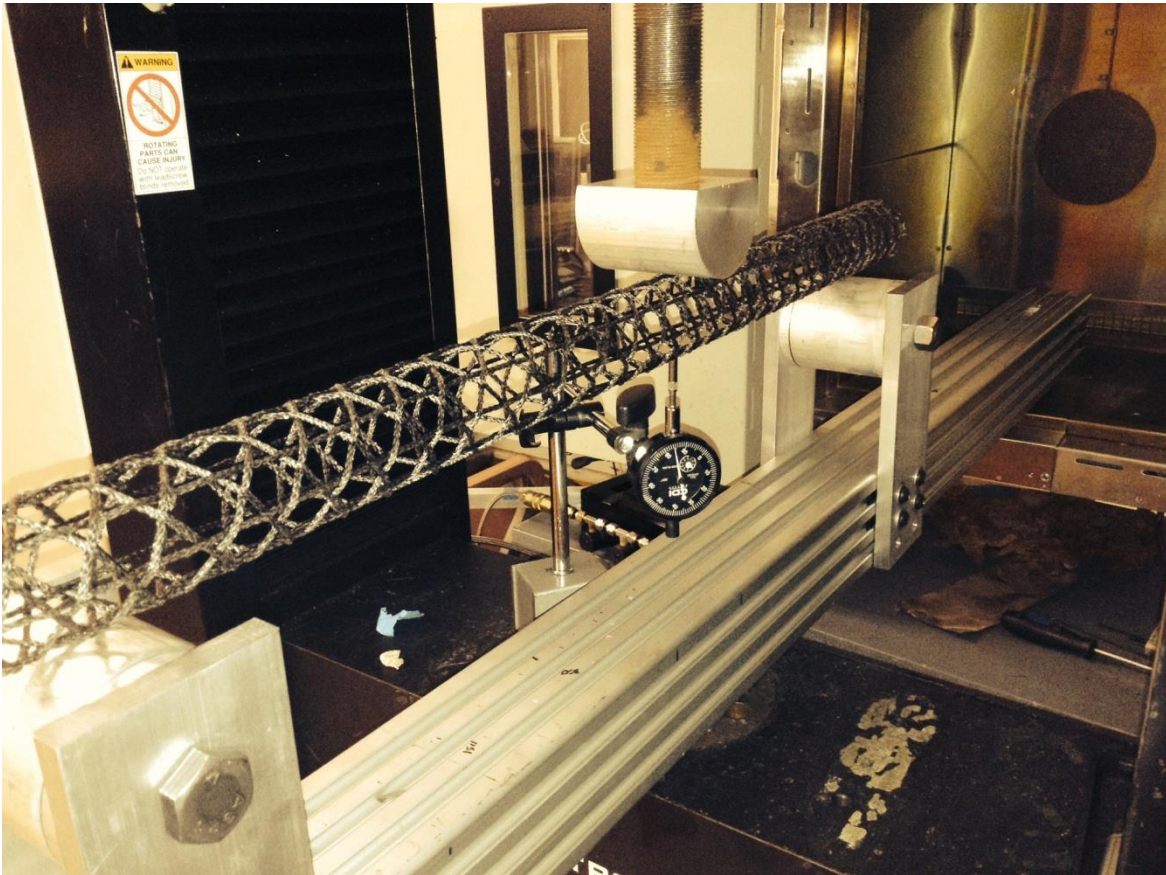


Figure 13 Three Point bending test on O-ACS tube

The top deflection was obtained from the readings measured by the Universal testing machine while the bottom deflection was recorded using a dial indicator. The force-deflection curves obtained for the top as well as the bottom readings from this test are shown in the Figure 14

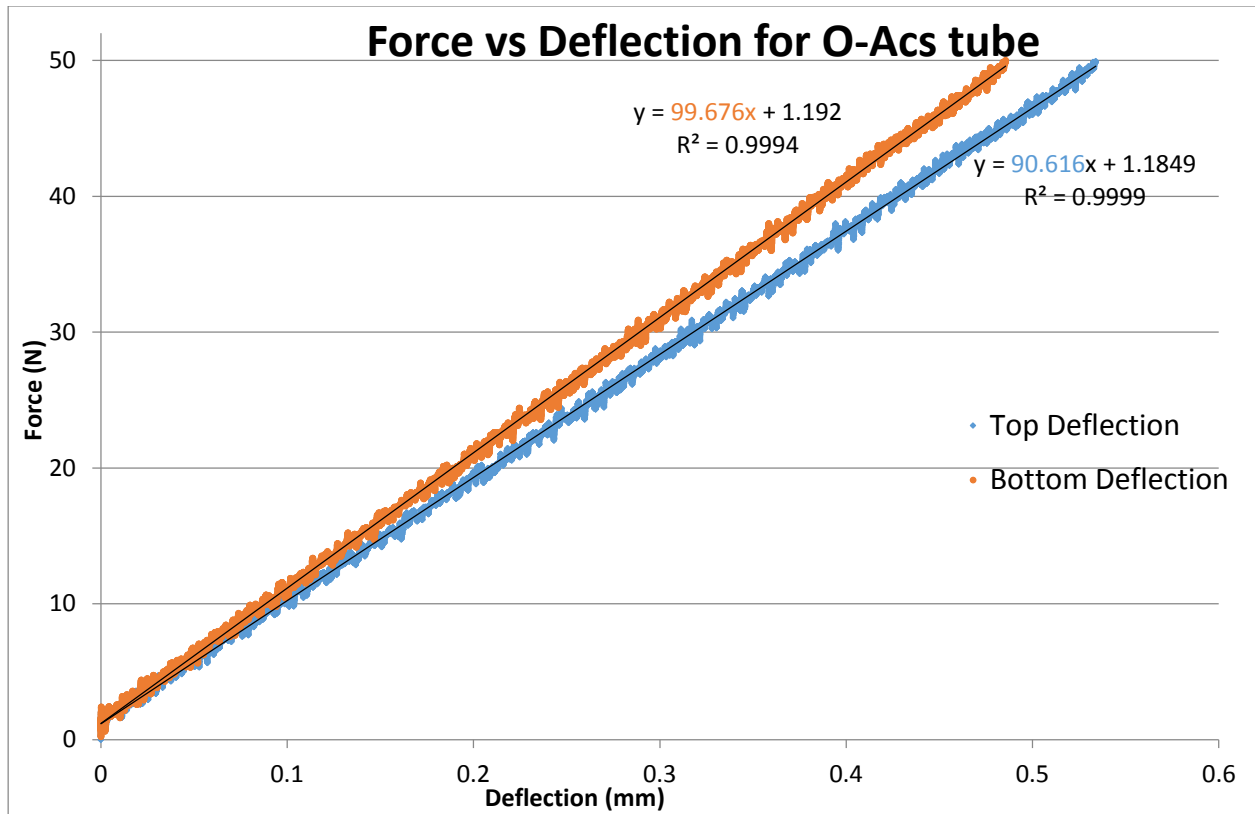


Figure 14 Force - Deflection curves measured at the top and the bottom of the O-ACS

From the above force-deflection plot it can be inferred that there is localized deflection at the point of loading which leads to more deflection at the top of the tube than at the bottom, at the loading point. It is due to this larger deflection at any given force that the stiffness (slope of the force-deflection curve) is lesser when read by the testing machine than the one obtained using the dial indicator. This would lead to inaccurate measurement of bending stiffness. There is a possibility of having such localized deflection at the contact points at the supports as well.

The Aluminum tube was then tested in a similar fashion and is illustrated in the Figure 15. The Force deflection curves obtained for this test from the top and the bottom readings are show in the Figure 16.

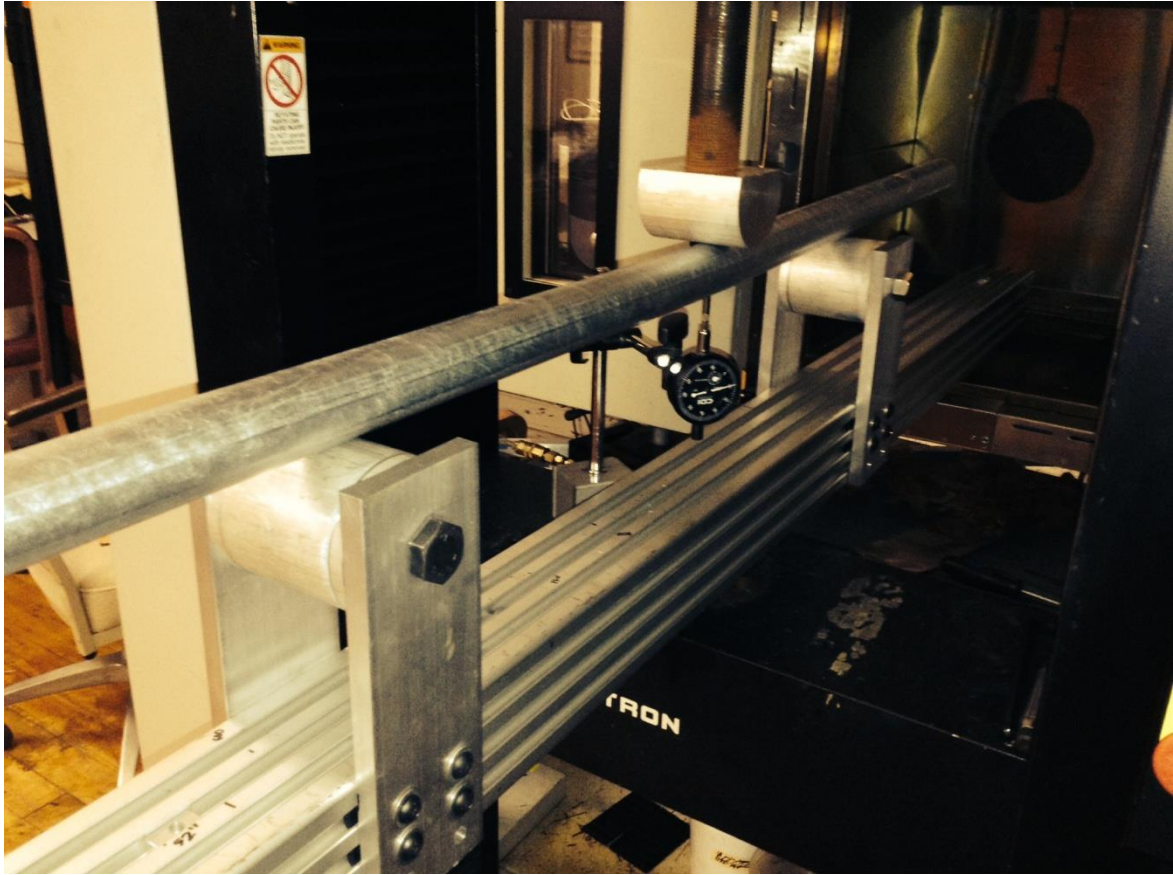


Figure 15 Three Point Bending Test on Aluminum tube

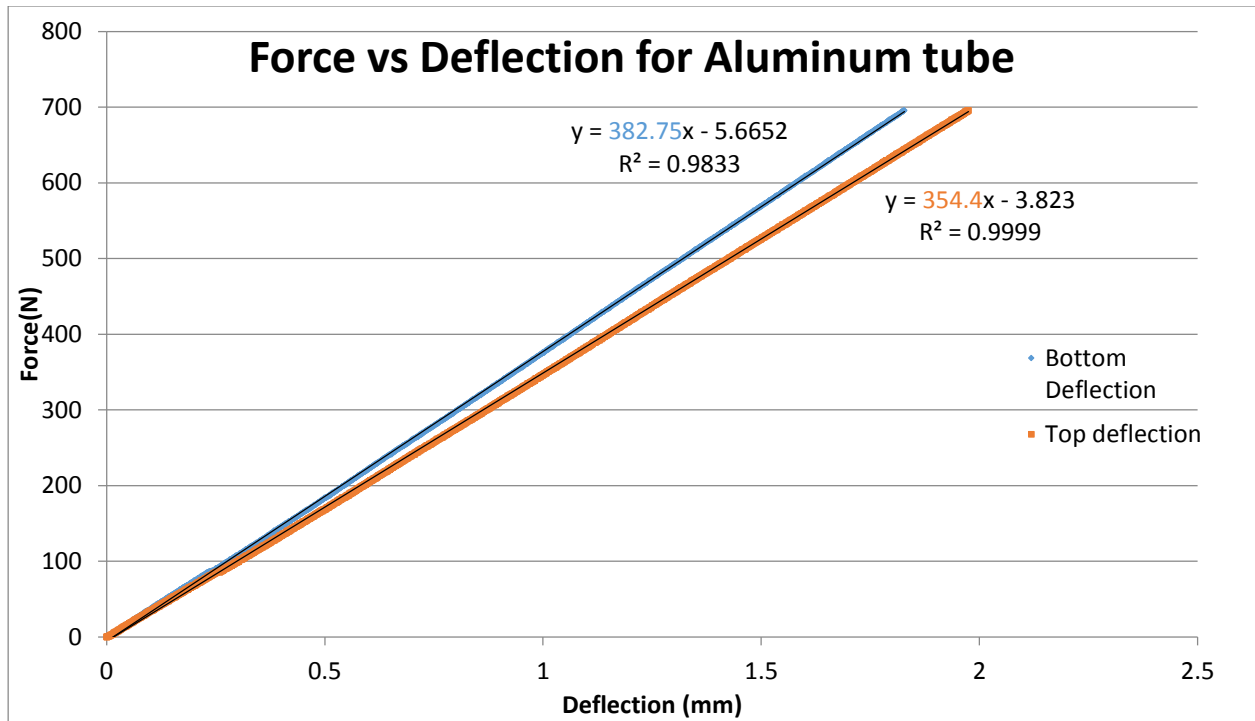


Figure 16 Force - Deflection Curves measured at the top and the bottom of the Aluminum tube

Similar results were obtained for the aluminum tube as for the O-ACS tube; showing that the thin walled aluminum tube also deforms locally. More deflection is thus obtained at the top than at the bottom leading to inaccurate measurement of stiffness.

Modified Three Point Bending Test

To reduce the localized deflections under the nose and at the supports, collars were clamped tightly on to the tubes which would prevent them from going out of round. The tests were performed again with the collars clamped at the loading point and at the points of support and deflections were measured at the top and the bottom of the collars. Two piece clamp-on shaft collars were used so as to compensate for any slight variations in the diameter of the test specimens. The collar dimensions are shown in the Figure 17

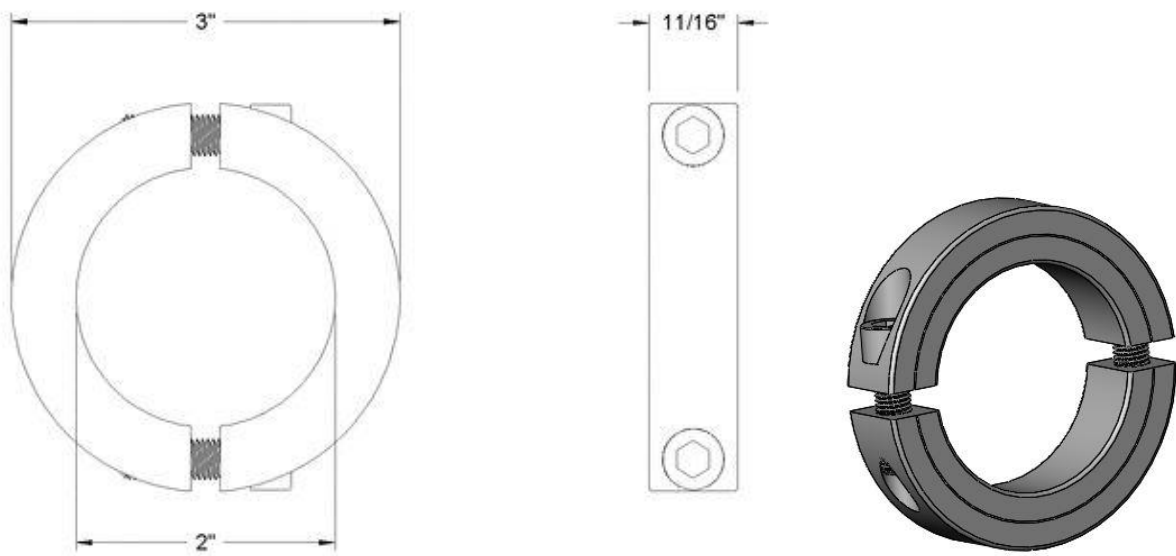


Figure 17 The Front view, Side view and the Isometric view of the Collar

Validation

The modified three point bend test with collars was then validated using the aluminum tube first, before testing the open structure. The aluminum tube was tested in 3 point bending using collars and the deflection was measured both at the top and the bottom (See Figure 18). There was no difference found in between the top and bottom deflection which is quite obvious as the collar is rigid and cannot go out of round, but this proves that our deflection measurement techniques are accurate.

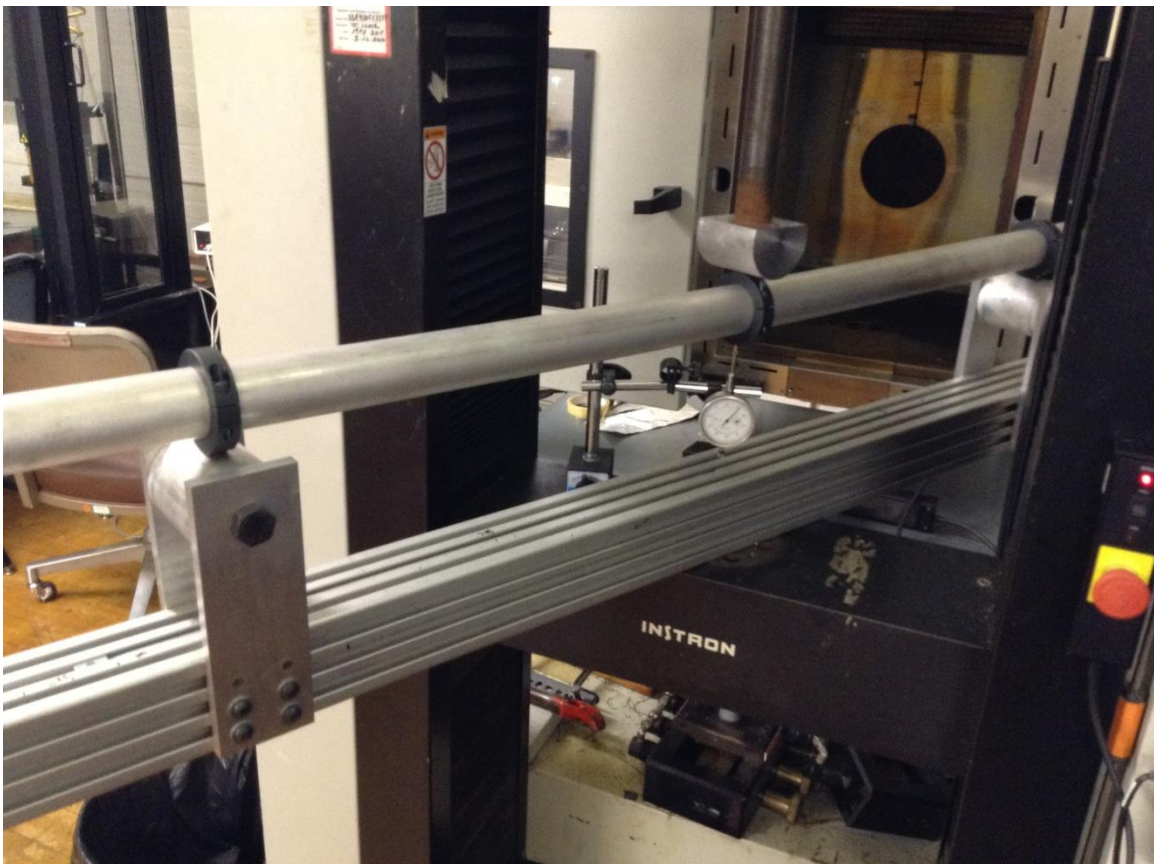


Figure 18 Aluminum tube while testing in three point bending with collars

Effect of collars on the bending stiffness of specimens with varying span lengths

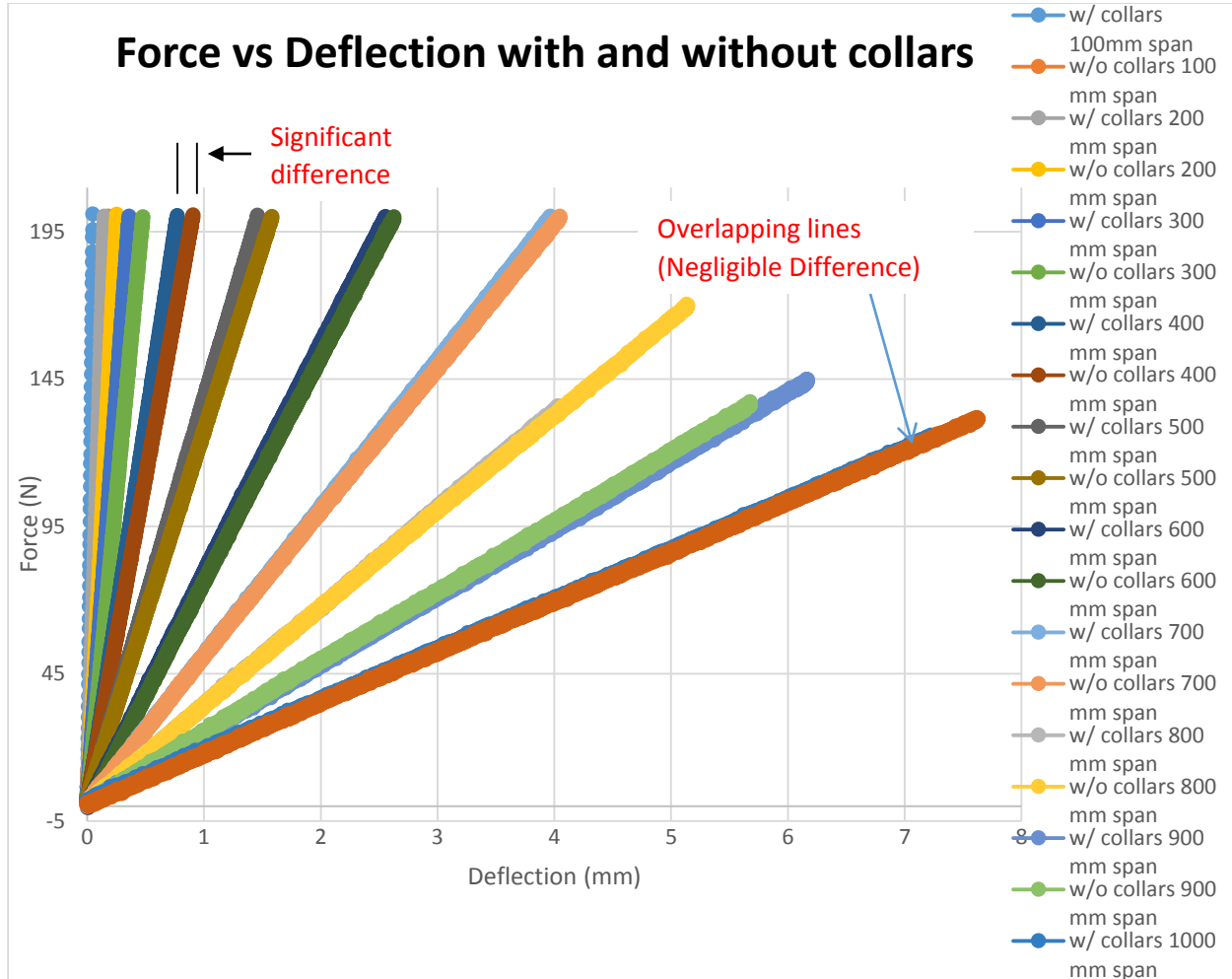


Figure 19 Force-Deflection Curves on Aluminum tube with and without collars

The aluminum tube was tested at varying span lengths ranging from 100 mm to 1000 mm, with and without collars and the results obtained are shown in the Figure 19. It can be seen that the stiffness with collars was always found to be more with the collars than without them. Also the difference is considerable for shorter span lengths and reduces with increase in span length and for the 1000 mm span it is negligible and the force-deflection curves overlap.

The bending stiffness should ideally be independent of the span length but due to the deflection arising from shear force and from contact stresses, the span length has to be of a certain minimum length at which the deflection due to forces other than bending moment forces can be considered negligible. At this point the bending stiffness (EI) (experimental) should match the calculated bending stiffness, for materials whose Young's Modulus (E) is known and the specimen's inertia (I) can be calculated. After this point the bending stiffness (EI) should not change with any further increase in the span length. Thus a bending test method can be validated when the bending stiffness (EI) stops varying with increases in span length. The aluminum tube was tested at varying span lengths from 600mm to 1200mm in steps of 100mm. The force deflection curves obtained for these tests are shown in Figure 20.

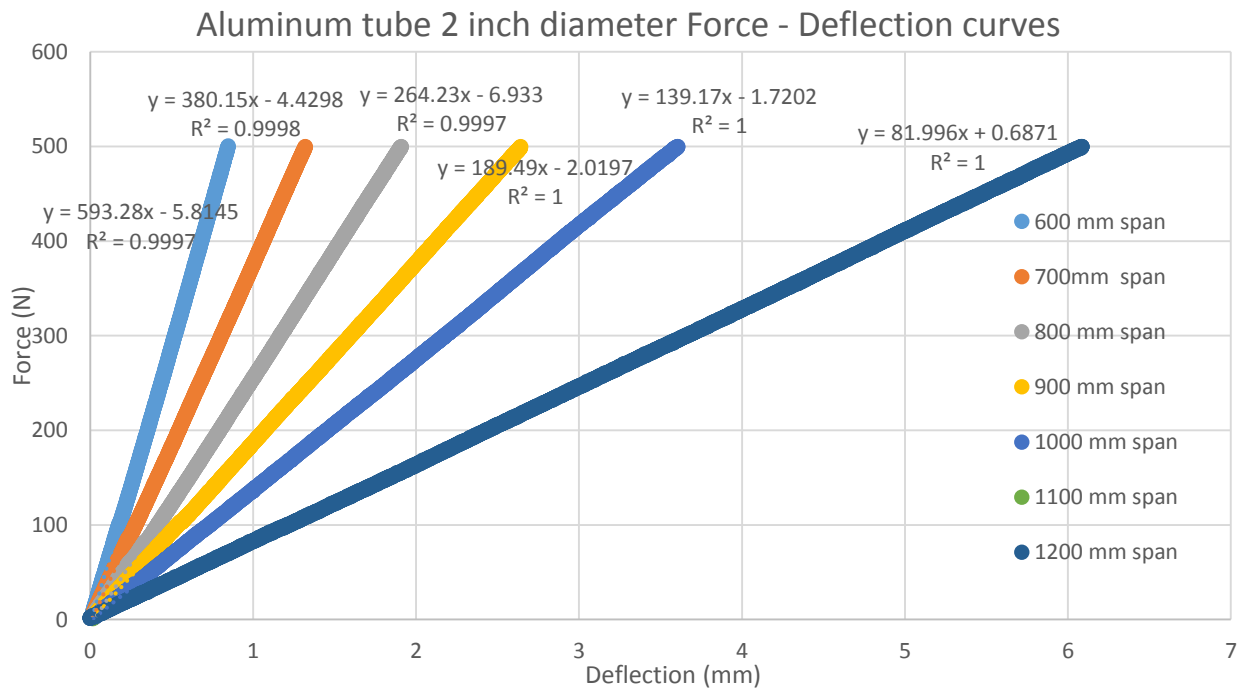


Figure 20 Force - Deflection curves of aluminum tube tested in three point bending with collars

The force deflection curves were straight lines with R^2 value of 1. The experimental bending stiffness was then calculated from these force deflection curves and plotted against the span length; the theoretical bending stiffness was also plotted for reference as shown in Figure 21. The following formula was used for calculating the bending stiffness (EI) values: $EI = PL^3/48 \delta$ [8]

Where P/δ is the slope of the force deflection curve at a given span length (L)

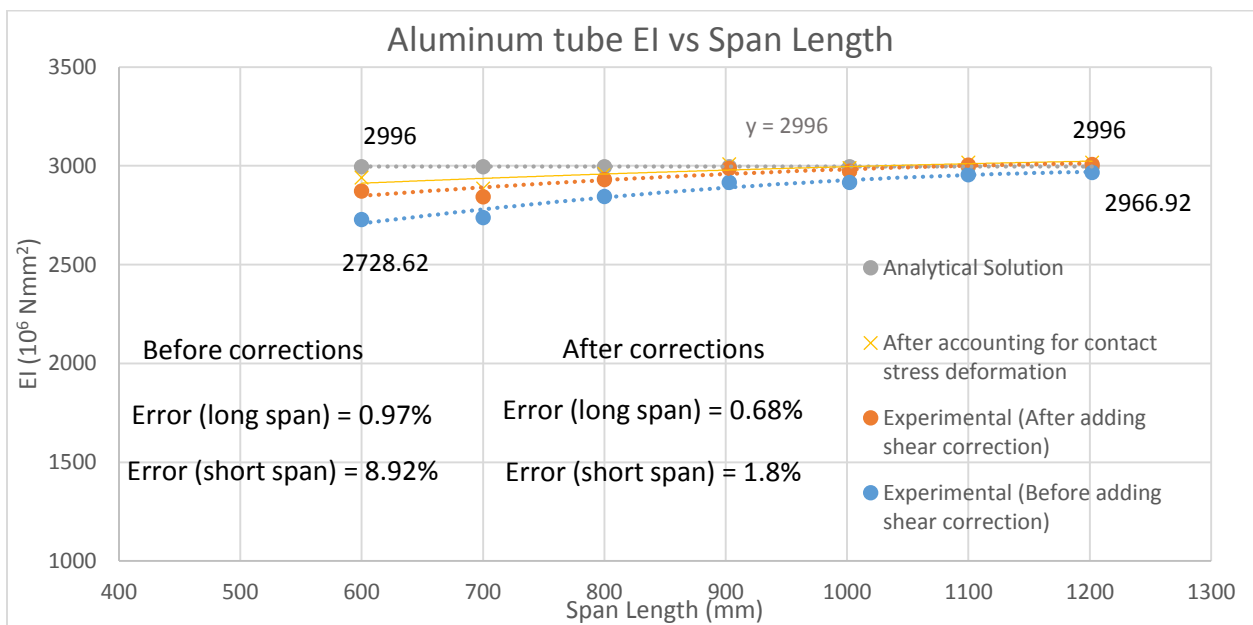


Figure 21 Variation in Bending Stiffness EI with changing span length

In Figure 21 the blue curve is the bending stiffness found experimentally while the green curve ($y = 2996$) is the theoretical solution for bending stiffness which does not change with span length. It is observed from the plots that there is larger difference in the theoretical and experimental values of bending stiffness for shorter spans and the difference keeps reducing with increase in span length. There is almost a 9% error for the shortest span (600 mm) and about a 1% error for the longest span (1200 mm). The reason for this difference in experimental and theoretical values

can be accounted for by calculating the effect of shear forces and contact stresses on the bending stiffness.

From Timoshenko's beam theory [9] the deflection due to shear is given by:

$$\delta_{\text{shear}} = PLc / 4AG \text{ [9]} \quad (1)$$

Where P is the load, L is the span length, A is the cross section area, G is the Shear Modulus, c is the Timoshenko shear coefficient (depends on geometry) The stiffness due to this shear deflection is given as

$$K_s = P/\delta = 4AG/Lc \text{ [9]} \quad (2)$$

The stiffness due to bending is given by

$$K_b = P/\delta = 48EI/L^3 \quad (3)$$

Eliminating the effect of shear

$$1/K_{\text{effective}} = 1/K_b + 1/K_s = K_s + K_b / (K_b \cdot K_s) \quad (4)$$

$$K_{\text{effective}} = (K_b \cdot K_s) / (K_s + K_b) \quad (5)$$

The bending stiffness after accounting for the shear effect will be

$$EI = K_{\text{effective}} L^3 / 48 \quad (6)$$

This gives the orange curve in the Figure 21. The corrected red curve is closer to the expected gray curve than the blue curve.

The deflection due to the contact stresses was calculated using the formula [9]

$$\delta_{\text{contact}} = 2Pc (1 - \nu^2) / \pi E [9] \quad (7)$$

Where E and ν are young's modulus and the Poisson's ratio.

After accounting for the deflection resulting from contact stresses the corrected bending stiffness was plotted against the changing span length on the same plot and is shown in the Figure 21 by the yellow curve. This curve is very close to the theoretical curve; with a negligible error for the 1200mm span length while less than 2% error for the shortest span (600 mm)

The test method can also be validated by measuring the deflection from bending, calculating the deflections due to shear force and contact stresses and comparing it to the expected theoretical deflection. Figure 22 shows the deflection with varying span lengths.

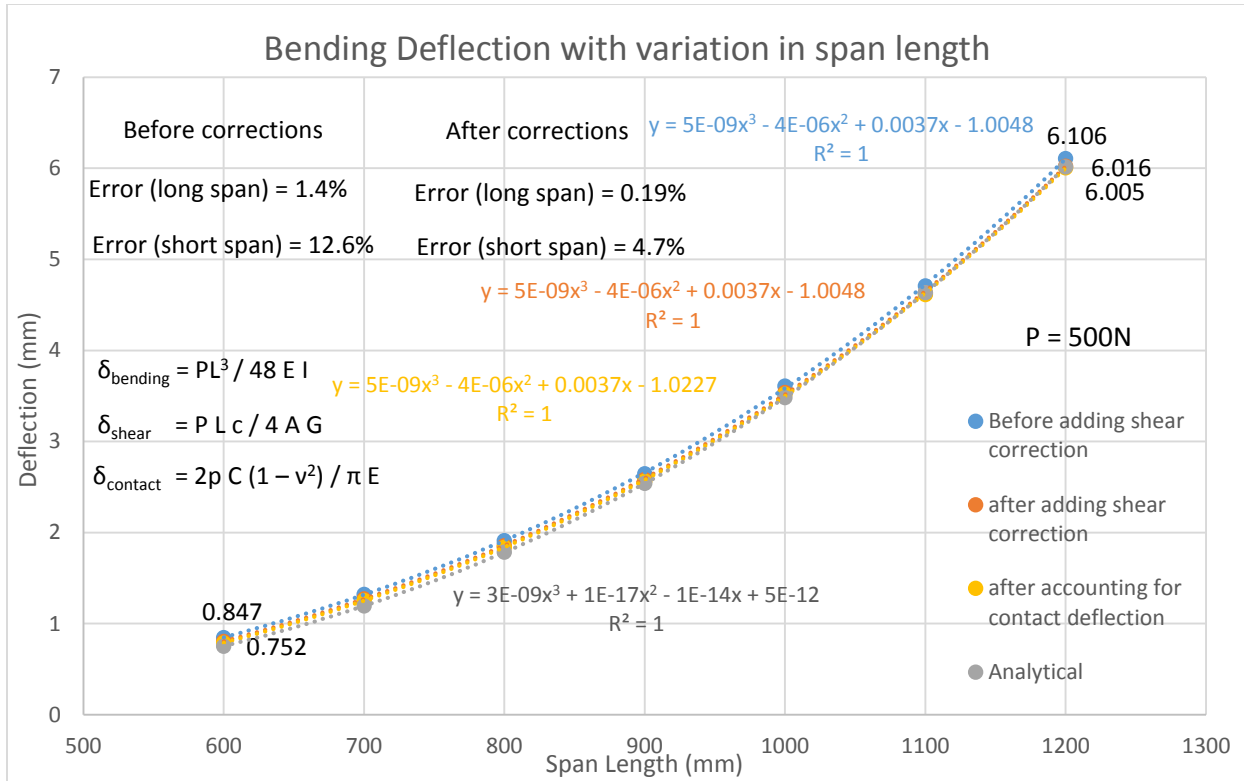


Figure 22 Comparison between measured deflection and analytical deflection and contribution of the correction factors required to eliminate to this difference

The theoretical values of deflection are shown by the gray curve in Figure 22 while the experimental values are shown by the blue curve. The experimental deflections are more than the theoretical as they include the deflections due to bending, shear and the contact deflections. After subtracting the deflection due to shear forces the effective bending deflections are shown by the orange curve in Figure 22. After further subtracting the deflections due to contact stresses the resulting deflections are shown by the yellow curve in Figure 22. The yellow curve almost overlaps the gray curve thus validating the test method.

Testing

Similar tests were performed on the O-ACS using collars at the loading point and at the supports as shown in the Figure 23. The Force deflection curves were obtained at the midpoint for varying span lengths and the results obtained are shown in the Figure 24



Figure 23 Performing modified Three point bending test on the O-ACS

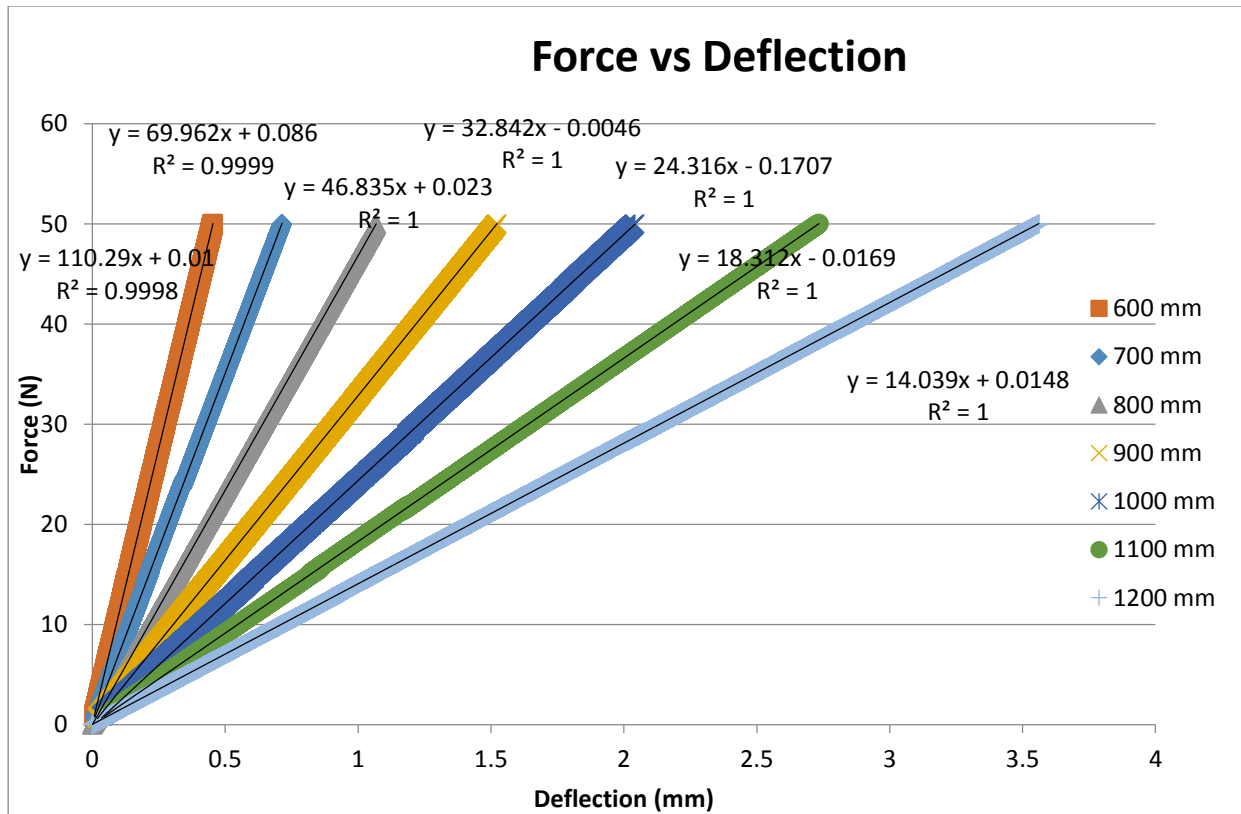


Figure 24 Force - Deflection curves from the modified three point bend test performed on O-ACS with fro different span lengths (600mm – 1200mm)

From these force deflection curves the bending stiffness was calculated for each span length and were plotted against the span length to observe the variation. The plot can be seen in Figure 25. Ideally, as discussed before, the bending stiffness (EI) should be constant and independent of the span length.

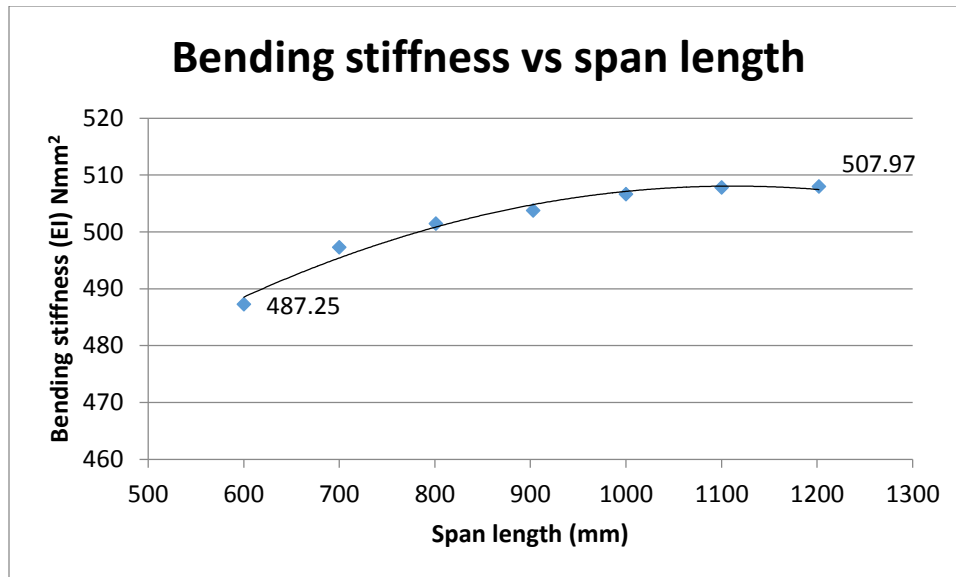


Figure 25 Variation in bending stiffness measured using modified three point bending test with changing span length

Similar to the aluminum tube the bending stiffness of the O-ACS was also found to be increasing with increase in the span length and starts to plateau out after a point. The reason for this being the same as in the previous experiment, that the contribution to the deflection due to shear and contact stresses reduces with increase in span length. In order to use the correction factors for shear and contact stresses, material properties like young's modulus and Poisson's ratio are required. These properties are not available for O-ACS. Also constants used in Timoshenko beam theory are shape dependent and determining these constants for O-ACS is very complex. Therefore in order to get accurate results long tubes about 1200 mm (≈ 24 times the diameter) need to be tested. This would mean to test samples which are 2.5 in or 3 in, sample lengths would have to be more than 5 feet or 6 feet respectively. This would also mean that a test rig to accommodate these long specimens would have to be built. For an optimization study where a large number of samples need to be manufactured and tested this would require tremendous labor and time. Another problem with this

test method is that the collars don't adhere to all the yarns equally due to the undulations and therefore, even though the load is not concentrated on 1 yarn or joint, it is not distributed equally.

Conclusions

Though, by using this method it is possible to find approximate bending stiffness of the O-ACS quickly, even by using short specimens, in order to get accurate results extremely long specimens and test rigs are required. The shortcomings revealed of the modified three point bending test, led to the necessity of developing a new test method in which there would be no contribution to the deflection due to shear and contact stresses and be purely bending.

Consideration of Standard Four Point Bending Test

The Four point bending test is believed to have pure bending in the middle section between the two loading noses. Using this, the errors due to shear deformation can be reduced but the contact stresses would still persist at the two noses and the two supports.

Pure moment test (Modified Four Point Bending Test)

In order to have no contact stresses and have pure bending a new test method was developed. This method is referred to as pure moment test in the following parts of this thesis. The idea behind this test method is to have extensions attached firmly (potted with epoxy) to the test specimen on both ends and to apply the load on these rigid extensions instead of on the specimen itself. The solid model of the fixture with a test sample is shown in the Figure 26. The same two tubes (Aluminum and O-ACS) were used for testing

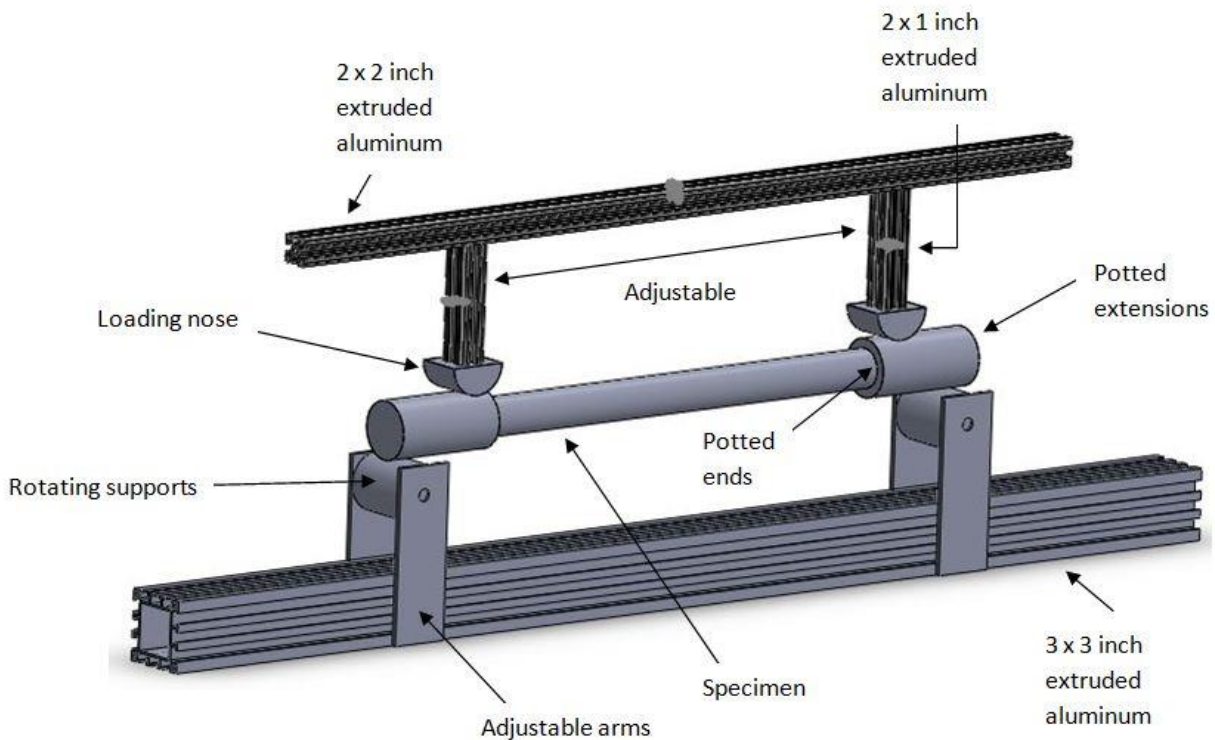


Figure 26 3D Model of the Assembled Pure Moment Fixture with an illustration of a specimen

Potting

The samples were potted with epoxy in 2 inch pipe nipples. 2 inch Pipe couplings were then screwed on to these nipples to make extensions. To have more extension, 2 couplings were attached on both sides using nipples to connect the couplings. The details of the nipples and couplings are shown in the Figure 27. The epoxy used for potting was 635 Thin Epoxy Resin by US Composites along with a 3:1 epoxy hardener. Figure 28 shows a picture of the epoxy resin and hardener used for potting.



Figure 27 Drawings and specifications of the nipples and couplings used for potting



Figure 28 Epoxy resin and hardener used for potting

Alignment of the specimen axis with the axis of the nipples in which it is potted is extremely important. For this reason the potting was done very carefully using a special fixture. The nipples are tapered and therefore were first attached with collars. The specimen was held with these nipples and collars at each end. The collars were then strapped to a rectangular rod with a V-groove in it for alignment and then filled with resin one side at a time. The Figure 29 [2] shows step wise procedure for this set up. “Because epoxy should not be allowed to jam in the coupler threads, a sheet of plastic vacuum-bagging material is used to keep the epoxy from leaking. Step 1 shows the necessary materials: Pipe nipple, pipe coupler, plastic sheet, and rubber band. Step 2 is to thread the coupler and nipple together with plastic sheet between: this will contain the resin. It was found to be very helpful to glue the sheet in place first with (e.g.) superglue to prevent resin leakage. In Step 3, the rubber band is used to support the free ends of the plastic, which can be trimmed as

desired at this point. The two end caps ready, Step 4 shows the fixture; the ends of the structure are wrapped with a cloth material to evenly space it from the walls of the nipple and keep it aligned therewith. Finally, Step 5 shows the fixture completed; the couplers are bound to the rod with (e.g.) hose clamps, the fixture is placed in a vertical orientation, and the ends can be subsequently potted. It is desirable that the rod have a channel in it to help align the couplers. The sixth step is the finished sample, ready for testing.” [2]

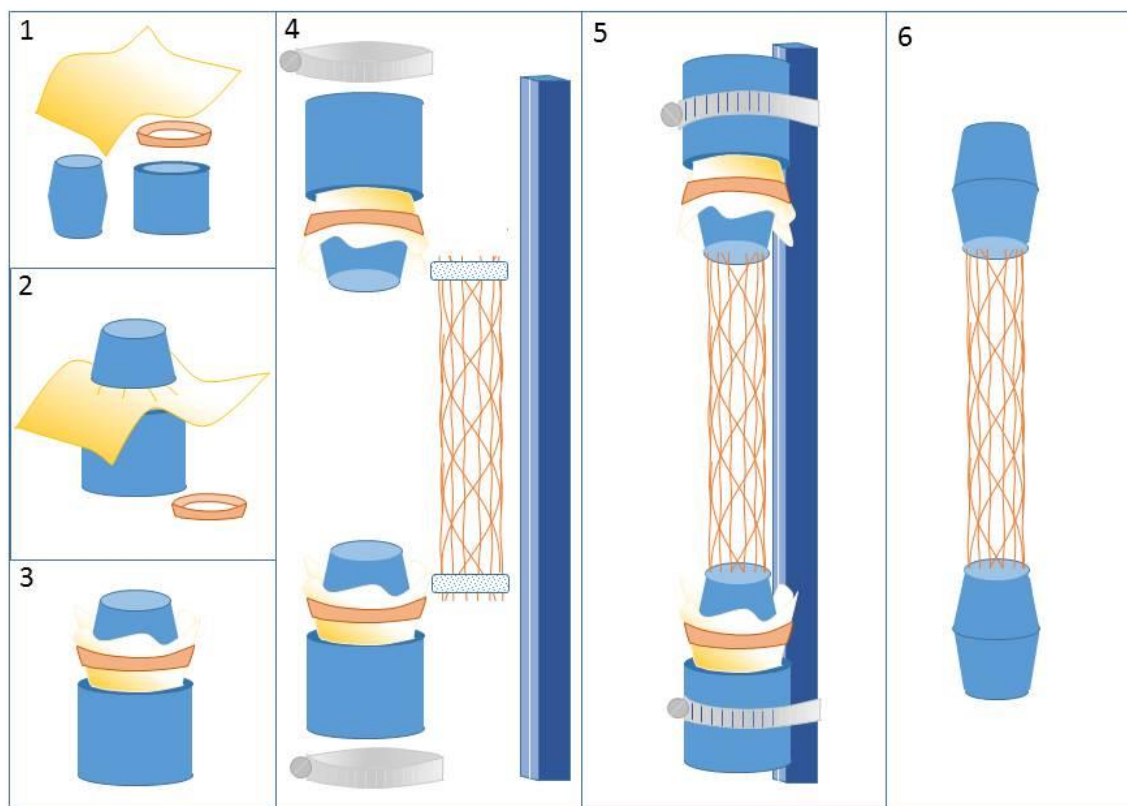


Figure 29 Stepwise procedure for potting the specimen [2]

Figure 30 shows a picture of the aluminum tube while potting while Figure 31 shows the O-ACS being potted using the alignment fixture.



Figure 30 Potting the ends of the Aluminum tube



Figure 31 Potting the ends of the O-ACS

Validation

The aluminum tube was first tested with varying span lengths on the pure moment fixture for spans 1000 mm to 600 mm. Figure 32 shows the potted aluminum tube while testing on the pure moment fixture. A load cell on the top cross beam was used to record the force applied quasi-statically and

the displacement of the lower cross beam was also recorded every 0.05 seconds. The rate of the test was set to 1 mm/min.

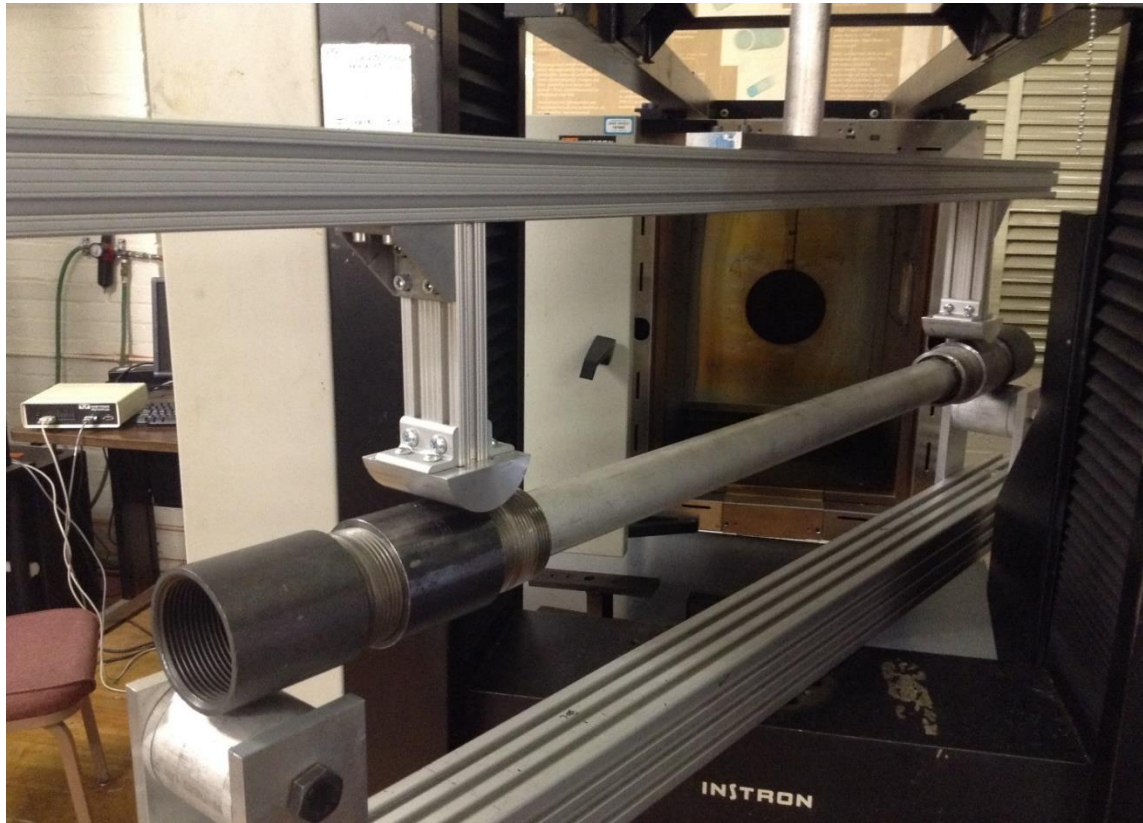


Figure 32 The Aluminum tube being tested in pure moment test

It was observed while testing that the fixture being of extruded aluminum is also bending considerably. A need was therefore felt to measure the compliance (reciprocal of the stiffness) of the fixture and subtracting that from the measured compliance of the specimen to get accurate data. Figure 33 shows an infinitely rigid steel channel used for measuring the bending stiffness of the pure moment fixture. The span length while measuring the stiffness of the fixture was kept the same as the span used for the corresponding test performed on the specimen. For all the tests

performed the distance between the loading noses and the end supports closest to them was set to a specific value (a) and was the exact same for both the sides to 0.01mm accuracy. A stencil was used to achieve this.

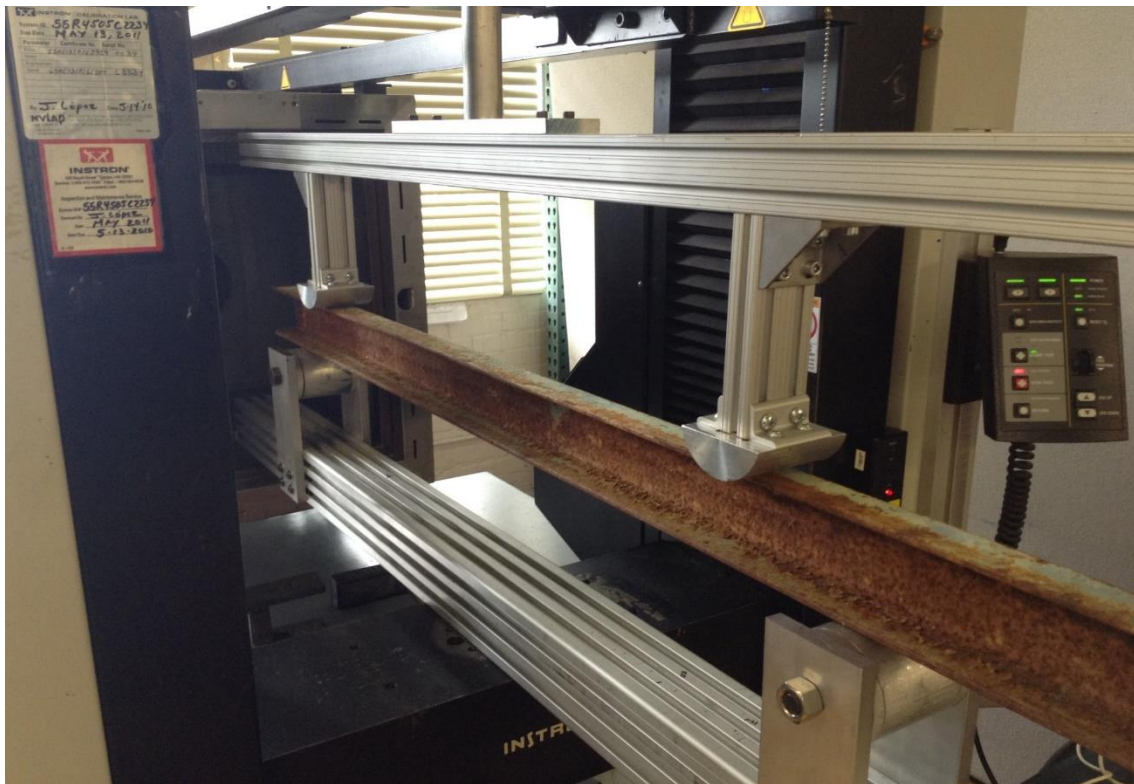


Figure 33 Measuring the Stiffness of the fixture

Calculations

Figure 34 aids in explaining the calculations done for obtaining the bending stiffness from the raw data provided by the universal testing machine. The load (P) and the deflection (δ) are obtained from the universal testing machine (Instron 5500). The span length is denoted by (L) and the

distance between each nose and the support end closest to it is denoted by (a). Points A and D are at the support ends while points B and C are under the loading noses.

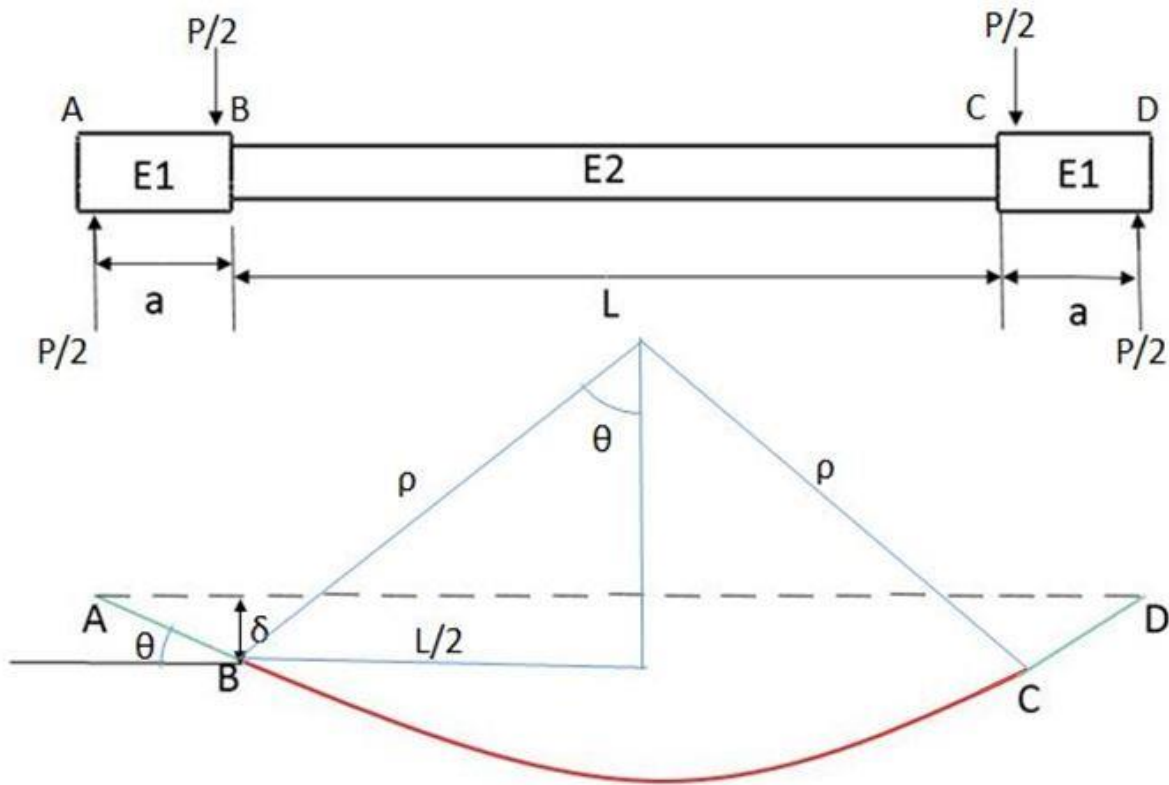


Figure 34 Geometric constructions to help in calculating the bending stiffness (EI)

Assumption: Slope of the line AB = Slope of the curve BC at point B

$$\sin \theta = \delta/a \quad (8)$$

$$\text{Also, } \sin \theta = L/2\rho \quad (9)$$

$$\text{Therefore, } \rho = La/2\delta \quad (10)$$

$$\text{From the bending theory } 1/\rho = M/EI \quad [9] \quad (11)$$

$$EI = M\rho \quad (12)$$

$$EI = MLa/2\delta \quad (13)$$

$$\text{We know, } M=Pa/2 \quad (14)$$

$$EI = Pa^2L/4\delta \quad (15)$$

$$EI = Ka^2L/4 \quad (16)$$

$$K = k1*k2 / (k2 - k1) \quad (17)$$

Where $k1$ = apparent stiffness of the structure (Specimen Test data),

$k2$ = stiffness of the fixture (Fixture Test data)

The Bending stiffness (EI) values thus obtained were plotted against the span length and compared with the analytical solution as well as the values obtained from the three point bend test. The importance of this study is to show that the pure moment test is independent of the span length and that it gives better results than the three point bend test if the correction factors were not available. Thus the values of EI from three point bend test used in this comparison are the values before they were corrected for shear and contact stresses. Figure 35 shows this comparison

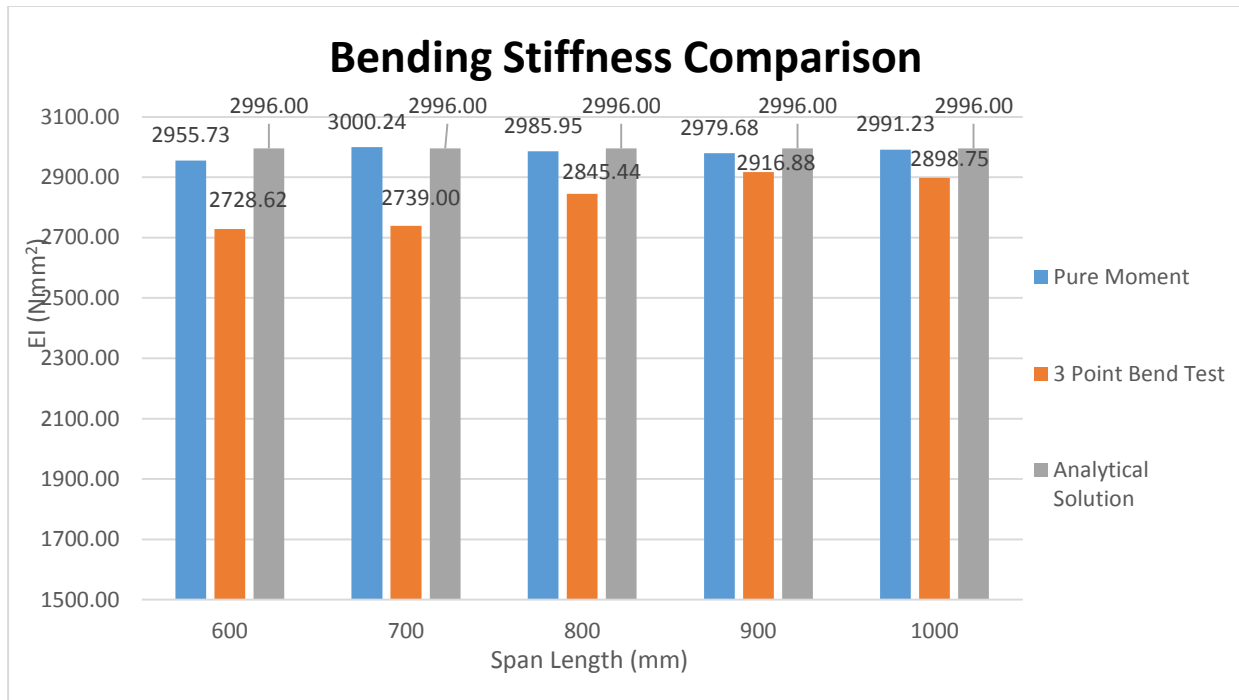


Figure 35 Comparison of bending stiffness values for aluminum tube obtained from the Pure Moment Test, from the Modified Three Point Bend test and from the analytical solution

The following observations can be made from the above chart:

1. The bending stiffness values resulting from the pure moment test are very close to the expected analytical solution (less than 1.5 % error)
2. The bending stiffness is not a function of the span length and the variation in the values are random, which might be due to other factors like slight inaccuracies in measurement of lengths, or the specimen and collars not being perfectly co-axial.
3. The bending stiffness results obtained by this method are closer to the theoretical values than the ones obtained from the three point bending test, thus proving that it is a better test method.

Testing

The O-ACS was also tested in a similar fashion for span lengths varying from 600 mm to 1000 mm in steps of 100 mm, the moment arm (a) was 100 mm for all the tests. Figure 36 shows the O-ACS being tested in the pure moment fixture. The O-ACS was oriented in the same fashion for all the tests performed in order to avoid variation in stiffness due to variation in the moment of inertia.

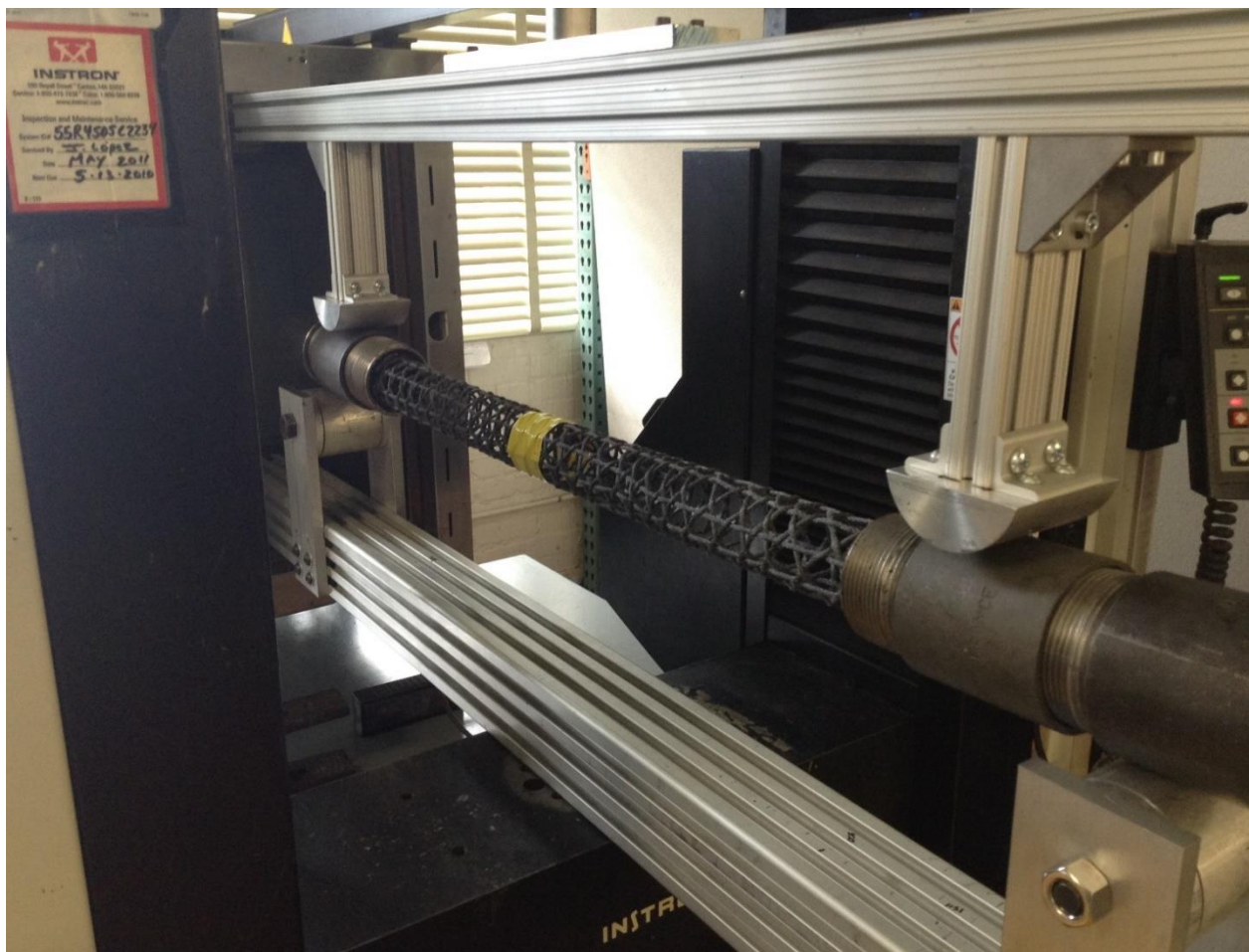


Figure 36 Testing of O-ACS using Pure Moment Test

The Force-deflection slope values (K) were obtained from the testing machine and the bending stiffness was calculated using the formula $EI = Ka^2L/4$. The stiffness of the fixture was measured

after every test to compensate for the deflection arising from it. The obtained values of bending stiffness were plotted against the span length and compared to the values obtained from the three point bend test. This plot is shown in the Figure 37

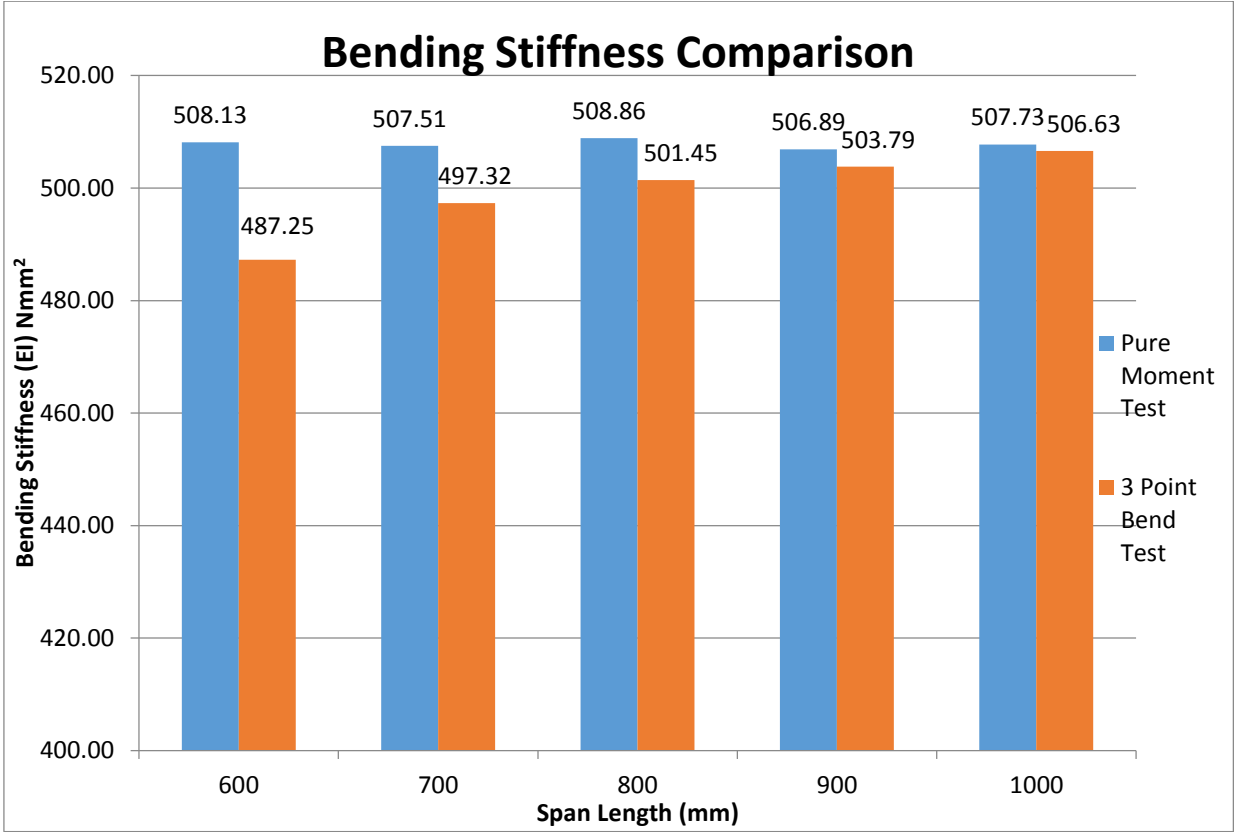


Figure 37 Comparison between bending stiffness values obtained from Pure Moment Test and Modified 3 Point Bending Test

The following observations can be made from the above chart

1. The bending stiffness values from the pure moment test are not a function of the span length and the variation in the values are random, which might be due to other factors like slight inaccuracies in measurement of lengths, or the specimen and collars not being perfectly co-axial, slight change in the orientation of the O-ACS tube, changing the moment of inertia
2. The bending stiffness results obtained by this method are more consistent and higher than the ones obtained from the three point bending test, which could be inferred to be a result of removal of deflection due to shear forces and contact stresses, thus proving that it is a better test method.

Advantages over Standard Bending Tests:

1. Shorter span lengths can be used for testing making it economical and faster
2. As it is pure bending the deflection due to shear is removed
3. No localized deflection
4. No contact stresses
5. Elimination of the need for a gigantic bending fixture

Conclusion

1. The Pure Moment Test (Modified Four Point Bending Test) was found to be an appropriate test method for measuring the bending stiffness of O-ACS as well as thin walled circular tubes.
2. Although, the Pure Moment Test is more accurate for instances where high accuracy is not required and the tolerances on the measured bending stiffness is higher than 5% the Three Point Bending Test with collars would be sufficient.

Compressive Stiffness and Modulus

Introduction

Structural elements in a truss are loaded in tension or in compression. It is therefore very important to know the ability of a structural element to resist such loads. The compressive *modulus* of a material gives the ratio of the compressive stress applied to a material and the resulting compression. Compressive modulus of a structural element, therefore, gives its ability to resist deflection while compressive stress is applied to it. We foresee the applications of O-ACS as structural elements in trusses and even other structures and therefore having a test method to accurately determine their compressive modulus is crucial.

ASTM Standards

ASTM E9-09 - Compression Testing of Metallic Materials at Room Temperature ¹⁰

This test method is performed using a well calibrated universal testing machine that conforms to the requirements of practices E4. Alignment of the vertical axis of the specimen and the direction of the force applied is very crucial; this is achieved in one of the following ways:

1. Machining the bearing surfaces parallel to each other within 0.0002 in/in
2. By using adjustable bearing blocks (Figure 38),
3. By using spherically seated bearing blocks (Figure 38)

A typical test set up has been shown in the fig (Figure 40)

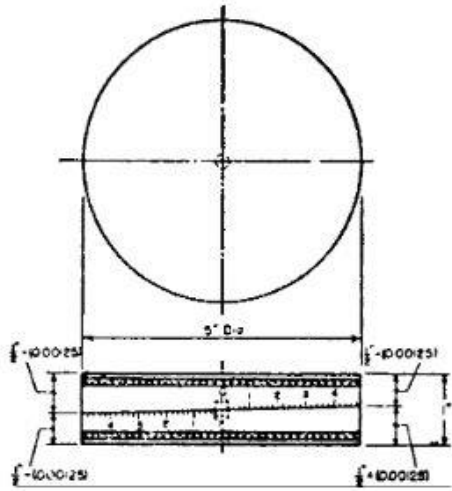


Figure 38 Adjustable bearing blocks [10]

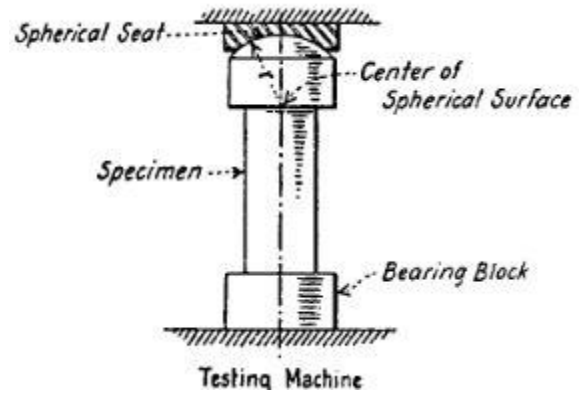


Figure 39 Spherically seated bearing blocks

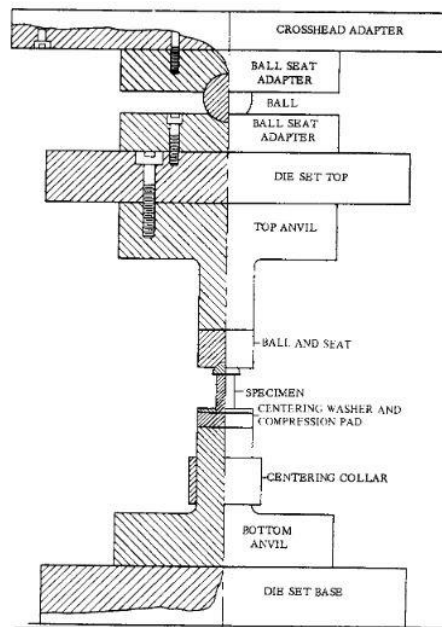


Figure 40 Example of a Compression testing apparatus [10]

ASTM D695 - Standard Test Method for Compressive Properties of Rigid Plastics ¹¹

“This test method covers the determination of the mechanical properties of unreinforced and reinforced rigid plastics, including high-modulus composites, when loaded in compression at relatively low uniform rates of straining or loading.” [11]

“The compression tool shall be so constructed that loading is axial within 1:1000 and applied through surfaces that are flat within 0.025 mm (0.001 in.) and parallel to each other in a plane normal to the vertical loading axis.” [11] Examples of a suitable compression tools are shown in the Figure 41 and Figure 42

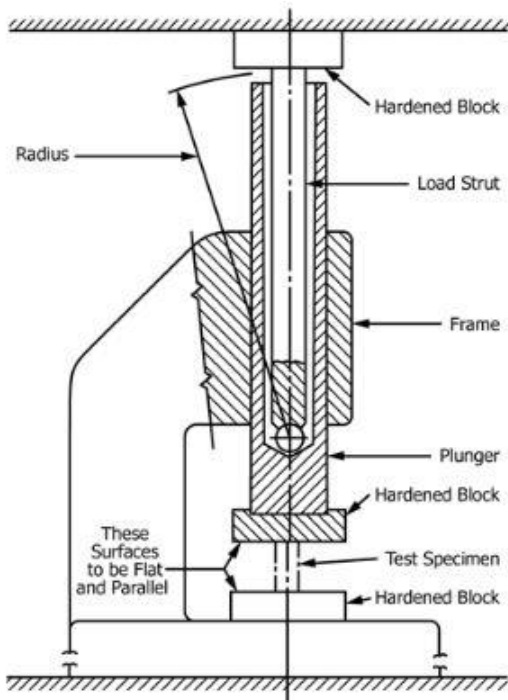


Figure 41 Sub press for compression tests

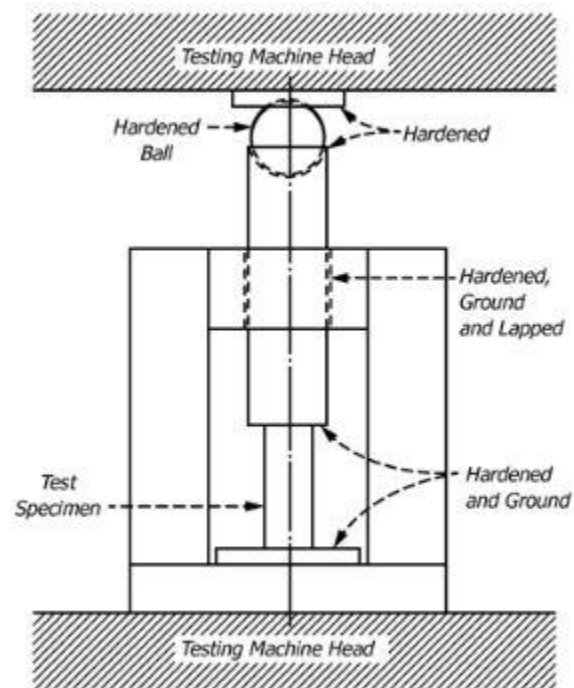


Figure 42 Compression tool

The aim of this section of the research is to develop a test method that accurately measures the compressive modulus of the O-ACS. After reviewing the standard test methods it was realized that it is of primary importance that the loading is purely axial. If the loading is not purely axial then, the specimen would be subjected to buckling and not purely compression.

The following ways were considered to obtain axial alignment:

1. Machining the bearing surfaces parallel to each other within 0.0002 in/in

Even if the bearing surfaces are machined parallel to each other within the specified limits, it is hard to make the 2 ends of an O-ACS tube parallel to each other, due to various reasons like vibration in the yarns while machining.

2. By using adjustable bearing blocks.

Adjustable bearing blocks make the bearing surfaces parallel but then again the problem of the tube ends not being parallel exists. If the ends of the tube are potted in end caps as in Figure 30 and Figure 31 then the adjustable blocks could be useful if the faces of the end caps are perfectly parallel to each other.

3. By using spherically seated bearing blocks

The ends of the O-ACS tube can be potted in end caps and spheres can be used in between these caps and the crosshead adapters for alignment. This method is much easier to implement than the adjustable blocks and therefore was adopted.

Test Setup

The O-ACS was first potted with epoxy in 2 inch pipe nipples as shown and described in Chapter 2 Figure 30. The 3D model of the test fixture is shown in Figure 43 and the actual fixture was built from the solid model and is shown in the Figure 44 and consists of the following:

1. Hardened spheres for alignment
2. A ball seat adapter having a spherical indentation to receive the sphere and threads on the other side to connect to the pipe nipple holding the specimen.
3. Another ball seat adapter which receives the sphere and has provision to be connected to the testing machine using a shear pin.

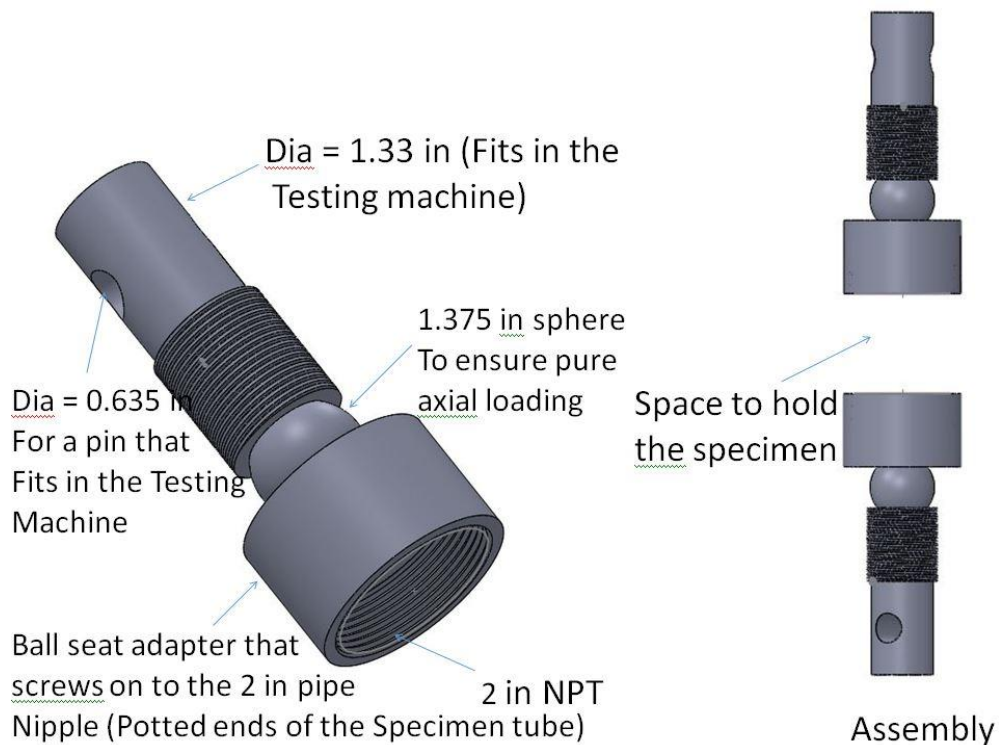


Figure 43 3D model of the compression fixture



Figure 44 Compression Test fixture

Validation

The test method was first validated using a 2 inch aluminum tube with the wall thickness 0.035 in. Figure 45 shows the potted aluminum tube and the tube being tested in the compression fixture. The specimen was loaded at a constant rate of 1mm/min and the force – deflection data was collected every 0.05 seconds to find the stiffness. Figure 46 shows this force deflection plot

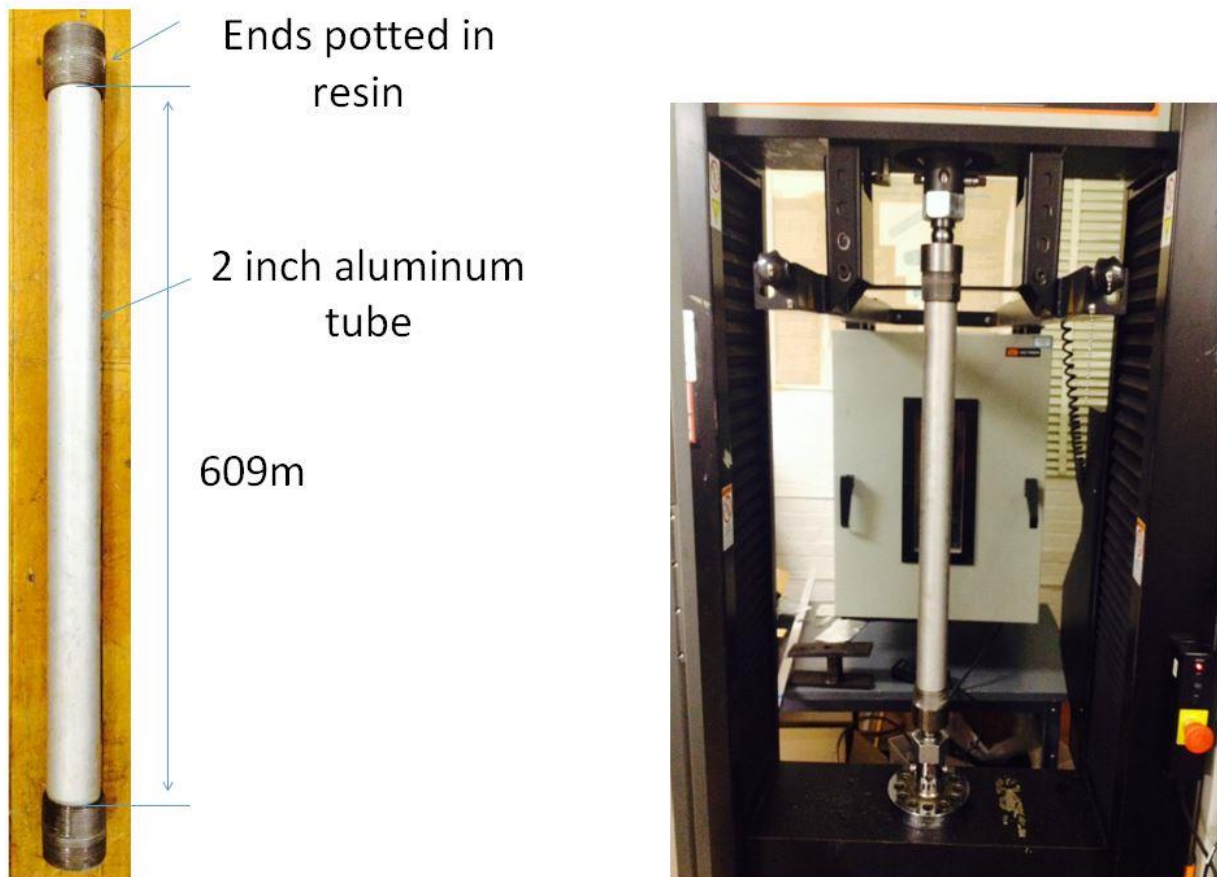


Figure 45 Aluminum tube with potted ends being tested in the compression fixture

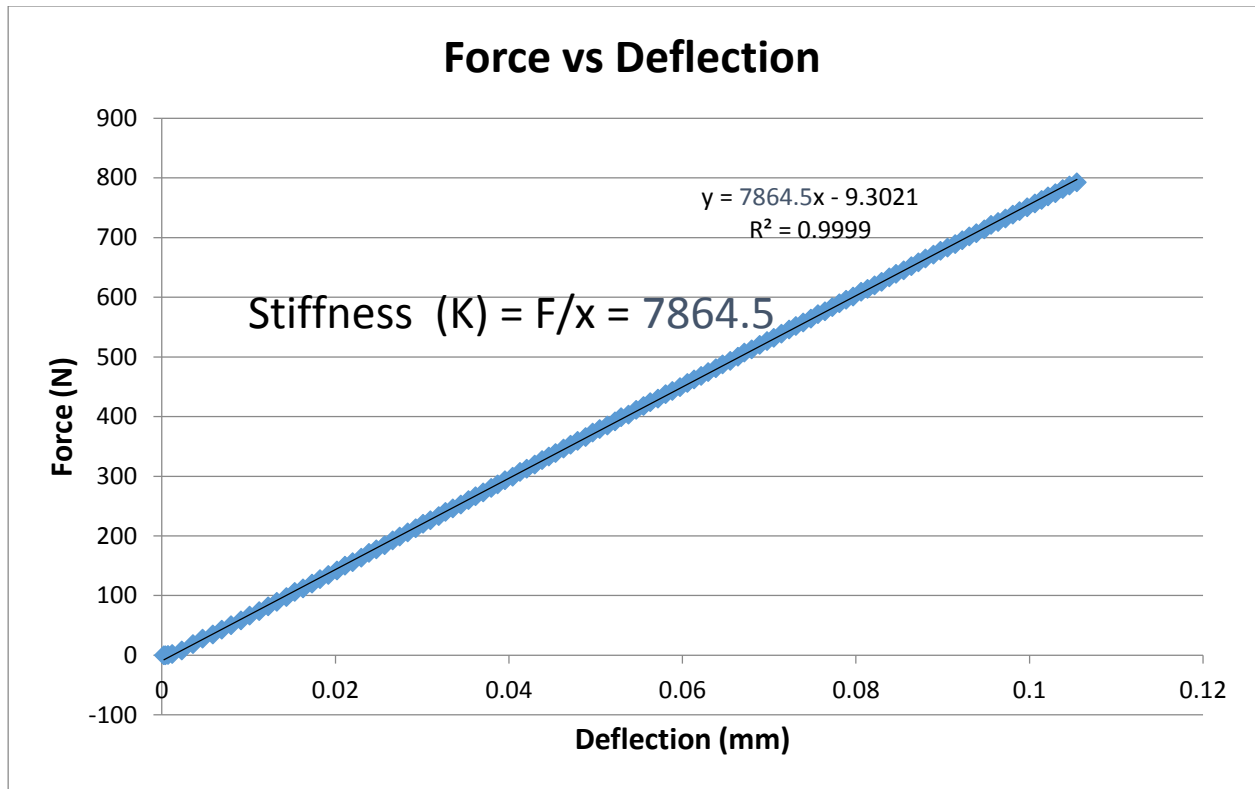


Figure 46 Force deflection curve from the compression test performed on the aluminum tube

This stiffness (K) is used to calculate the compressive modulus using the following formula:

$$\text{Compressive Modulus} = \text{Stress}/\text{Strain} \quad (18)$$

$$\text{Stress} = \text{Force (F)}/ \text{Cross sectional area (A)} \quad (19)$$

$$\text{Strain} = \text{Change in length } (\delta l) / \text{Original length (L)} \quad (20)$$

$$\text{Compressive Modulus} = F \times L / \delta l \times A \quad (F/ \delta l = K) \quad (21)$$

$$= K \times L / A \quad (22)$$

Thus by knowing the length of the sample and the area of cross section the compressive modulus can be obtained from the stiffness (K). The Figure 47 shows the comparison between the analytical and the experimental compressive modulus obtained by this test method.

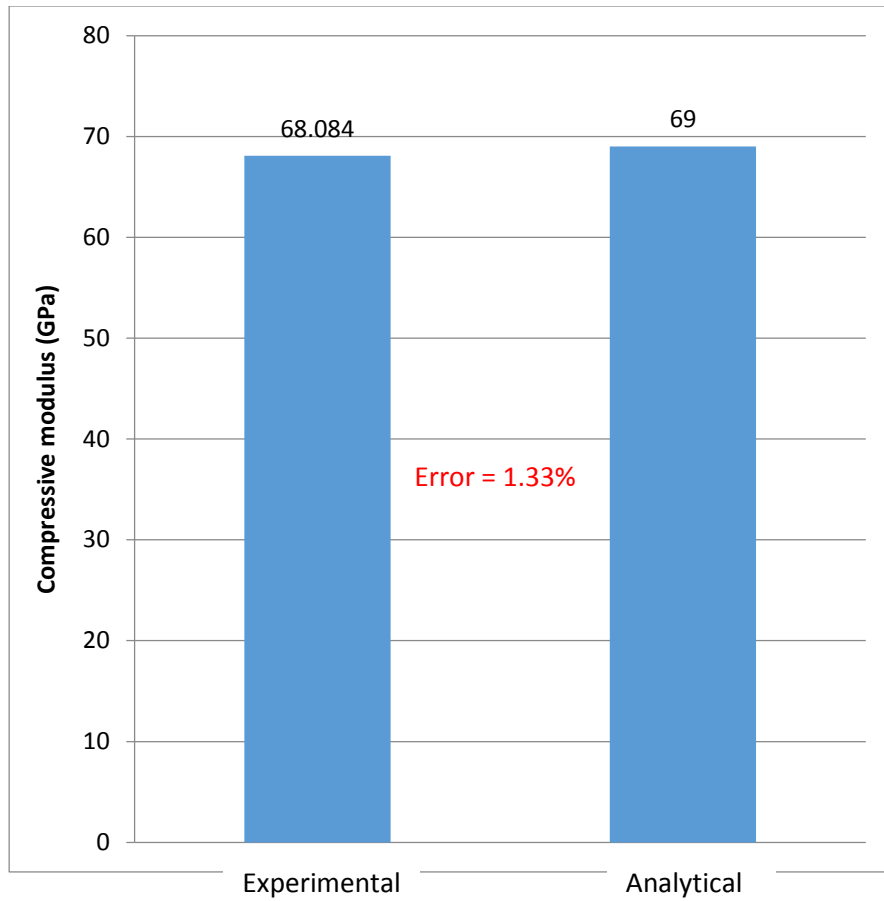


Figure 47 Comparison between the experimentally obtained compressive modulus and the analytical solution

The error in the experimental and the analytical value was found to be 1.33% which can be considered as negligible, and might have occurred due to slight misalignments between the tube and the nipple axis while potting or due to some impurities in the metal which would mean that the analytical value is not accurate. From this data we can safely conclude that the test method has been validated.

Testing

Several O-ACS were tested to find their compressive moduli and also a comparative study was carried in between different O-ACS with the parameters for comparison being compressive modulus and specific compressive modulus (Modulus per unit weight). The Aluminum tube was also considered in this comparison.

Table 1 describes the different configurations of structures tested, these structures were a part of an optimization study by Austin Gurley and the details can be found in “Austin Gurley, Design and Analysis of Optimal Braided Composite Lattice Structures” [2]

There are two changing parameters:

1. Braid angle (30/45/60)
2. No of axial yarns (4/8/12)

Table 1 Different configurations of O-ACS tested

Sample number	No. of axial yarns	No. of CW helical yarns	No. of CCW helical yarns	Braid angle	Length (mm)	Mass/unit length (gm/cm)
1	8	4	4	45	534	1.2
2	8	4	4	60	533	1.553
3	8	4	4	30	535	1.0587
4	12	4	4	45	537	1.446
5	4	4	4	45	533	0.957

The comparison between the first three tubes would give us an insight about how and how much does the braid angle affect the compressive modulus, while the comparison between 3,4 & 5 would provide us with information on how adding more axial yarns affects the specific compressive modulus of the O-ACS tube. The samples were mounted in the fixture as shown in Figure 48. All the samples were loaded at a constant rate of 1mm/min and the force – deflection data was collected to find the stiffness. Figure 49 shows this force deflection data for all the tubes

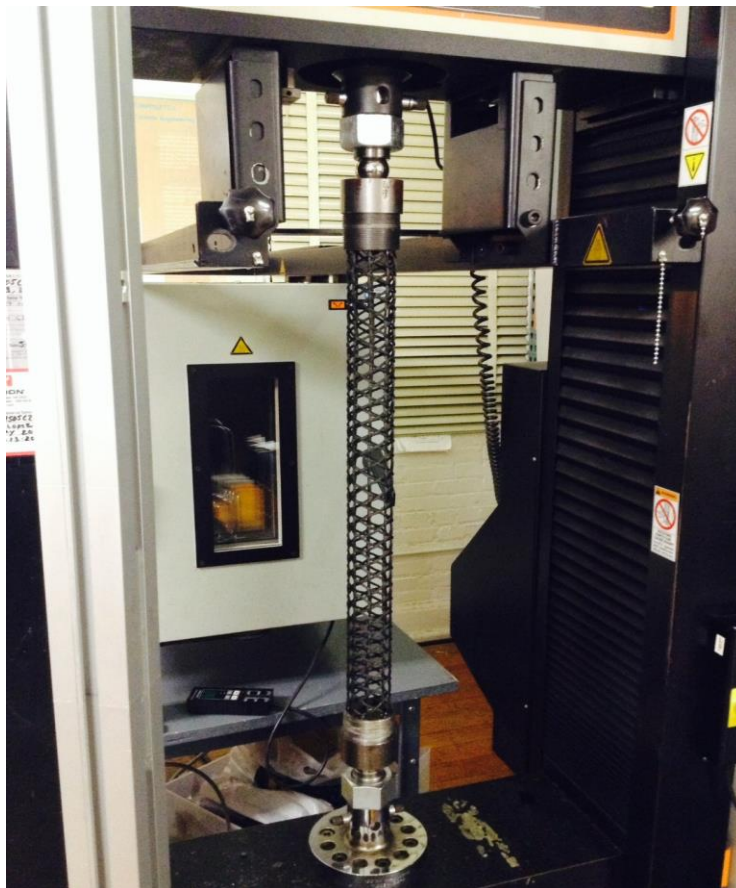


Figure 48 Testing the O-ACS in the compression fixture

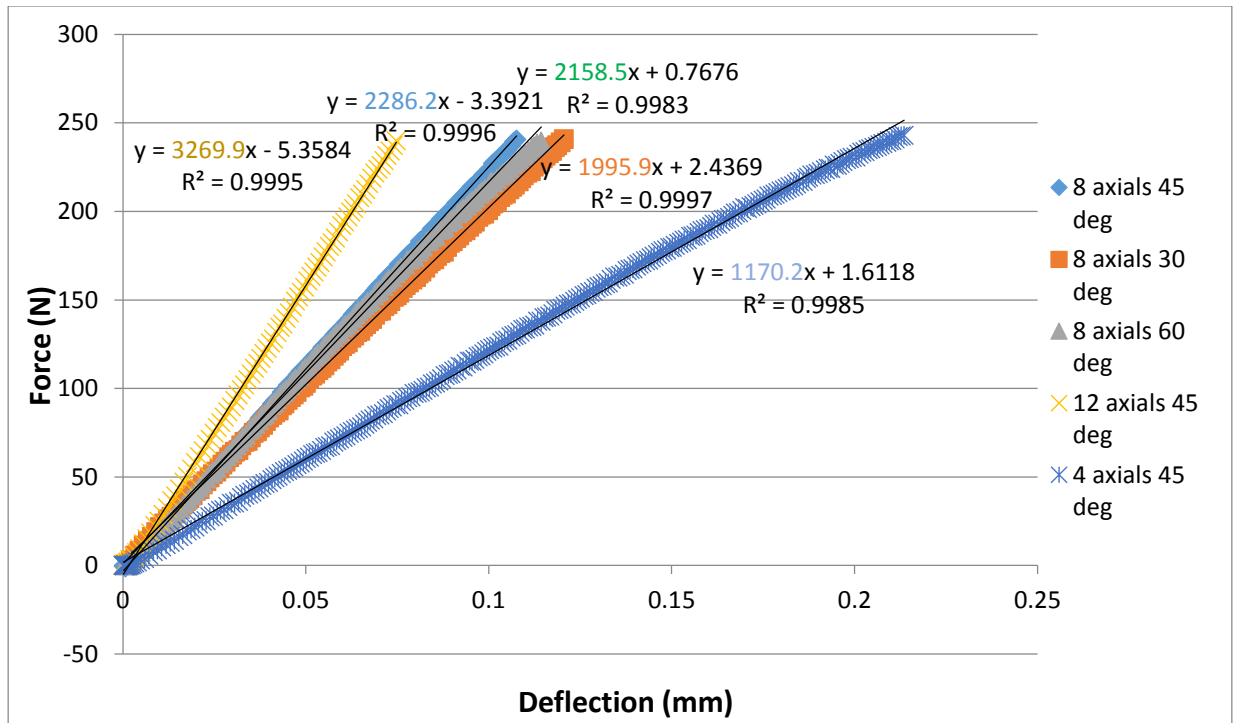


Figure 49 Force Deflection Curves of various O-ACS tested

It can be seen that for similar lengths the structure with 12 axial yarns deflects the least for a given load, while the structure with 4 axial yarns deflects the most. The structures with 8 axial yarns and varying braid angles have similar deflections at a given load, with not very significant difference.

Results

The Figure 50 shows a comparison between compressive stiffness K (Slope of the Force-deflection curve) of all the O-ACS tested. It can be seen from this plot that the number of axial yarns contribute largely to the compressive stiffness of the tubes while the braid angle has a small effect on the stiffness. The weights of the O-ACS tube are also varying and therefore a fair comparison would be the one where the specific stiffnesses (Stiffness/ (wt/ unit length)) are compared. The Figure 51 shows the comparison between the specific stiffnesses of the O-ACS

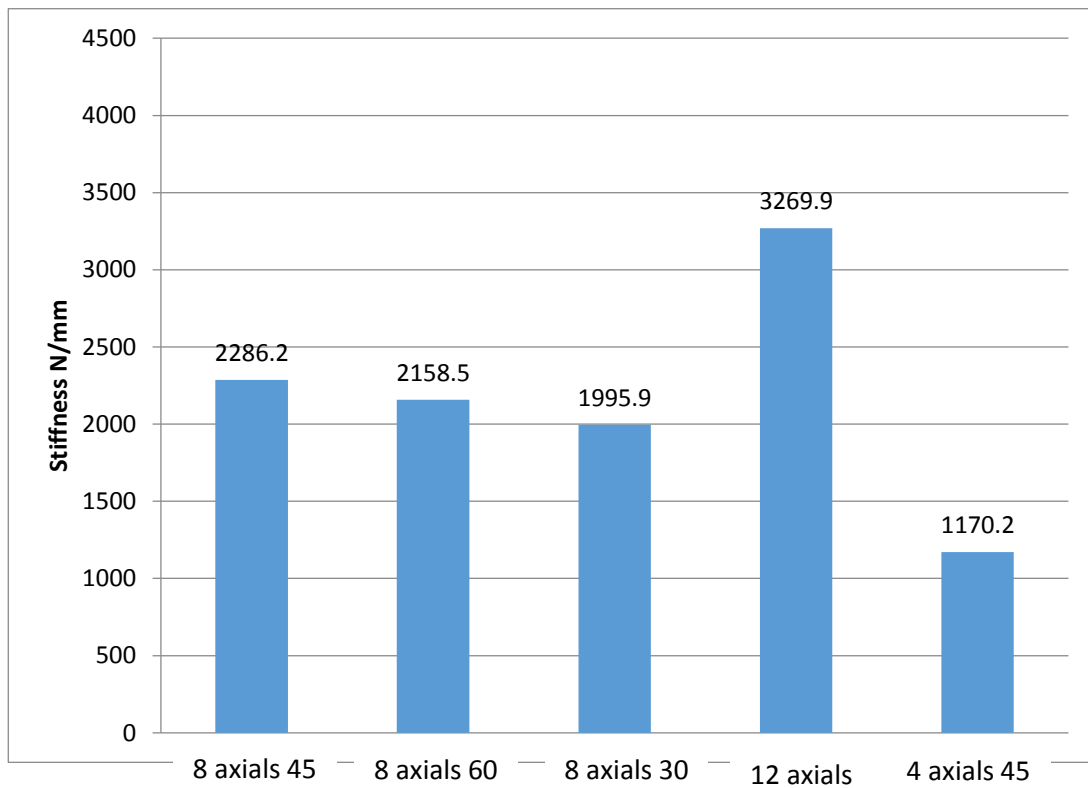


Figure 50 Comparison between axial stiffness of various configurations of O-ACS

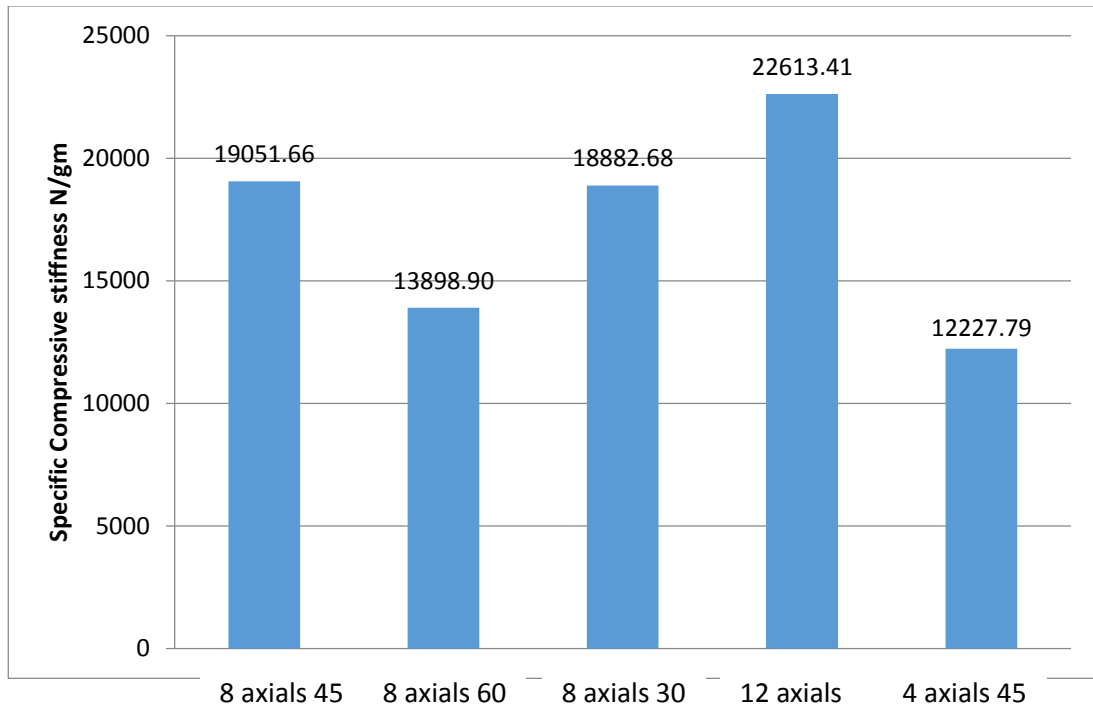


Figure 51 Comparison between axial specific stiffness of various configurations of O-ACS

It can thus be seen that the structure with 12 axials has the highest specific stiffness while the structure with 4 axial yarns has the lowest. In fact, the slope of the applied load vs the deflection is almost directly proportional to the number of axials (4 axials slope = 1170N/mm, 8 axials slope = 2286 N/mm and 12 axials slope = 3269 N/mm) Thus, by having more number of axial yarns high compressive stiffness/ weight ratio can be obtained in O-ACS. With the braid angle 30° the helical yarns contribute less to the compressive stiffness than when the braid angle is 60° but the amount of yarn used is much lesser, thus the specific stiffness is higher than that with the braid angle 60°. The braid angle 45° is optimum in between the 3 angles in consideration, as it has the right amount of yarn and with the angle 45° it provides sufficient resistance to the compressive loading.

From the stiffness data from Figure 51 the compressive modulus was obtained using the formula:

$$\text{Compressive modulus} = K \times L / A \quad (23)$$

Where, K is the stiffness from the force deflection plot, L is the length of the tube, A is the area of cross section

Assumption: The area of cross section was taken as the sum of the cross sectional areas of the axial yarns alone, as they contribute in resisting the compression the most while the helical yarns do not. It would not be fair to include the area of the helical yarns as they do not contribute significantly to the compressive stiffness. The Figure 52 shows the comparison of compressive moduli of all the O-ACS in this experiment.

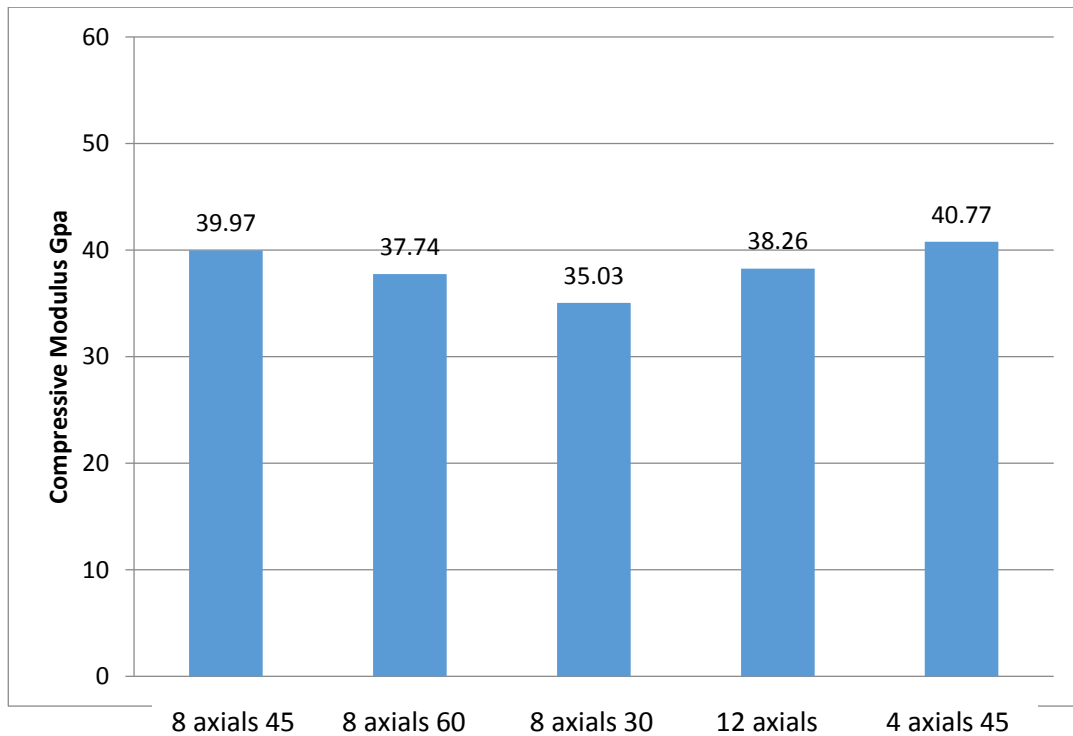


Figure 52 Comparison between compressive modulus of various configurations of O-ACS

The compressive moduli of all the structures are quite similar, which is what is expected, as we have now divided the stiffness by the area of cross section, which is nothing but the number of

axial yarns. As each of the structures had the same axial yarns, the compressive modulus should be the same. Any differences in the compressive modulus could be a result of discrepancies in the tubes while manufacturing or slight differences in the coaxiality of the structures and their respective end caps while potting.

Effect of Expanded poly propylene on bending stiffness of O-ACS

Introduction

Expanded polypropylene is a foam form of polypropylene. Polypropylene is a thermoplastic polymer. Polypropylene (PP) in the form of pellets is foamed using a blowing agent (CO_2) in a process tank to form foamed expanded polypropylene (EPP). Figure 53 shows a sample of polypropylene pellets while Figure 54 shows the expanded polypropylene beads formed from the pellets. EPP is used in various applications in the packaging industry, automotive industry and toy industry. For this experiment help from Hanwha Advanced Materials America was sought in procuring EPP beads as well as using their molding equipment.



Figure 53 Polypropylene pellets



Figure 54 Expanded polypropylene beads

O-ACS with EPP

One of the disadvantages of the O-ACS that were revealed while performing bending tests on them was that point loads applied on the O-ACS are not well distributed throughout the structure resulting in localized deflection and early failure of the O-ACS. An attempt was made in order to solve this issue by filling the O-ACS tube with EPP foam, which would maintain the structure's property of being light weight and still distribute the load around the circumference instead of just one yarn.

A one inch diameter O-ACS tube was braided over a mandrel on a 32 carrier braiding machine and was cured in the oven. The tube was cut into 2 parts and one part was filled with expanded polypropylene for a comparative study of bending stiffness. The tube was encased in a rectangular mold using supports to have it suspended in the mold (Figure 55 and below Figure 56). EPP beads were molded around and inside the O-ACS using a molding machine as shown in Figure 57. The excessive EPP around the O-ACS tube was torn off to leave a tube closely and completely packed with EPP beads. Figure 59 shows the O-ACS tube with EPP beads molded inside it while Figure 58 shows the other half of the tube without any EPP in it. The weight per unit length was increased from 1.549 gm/cm to 1.736 gm/cm after adding EPP to the O-ACS tube.



Figure 55 1 inch O_ACS held in supports to be placed in the mold of an EPP molding machine

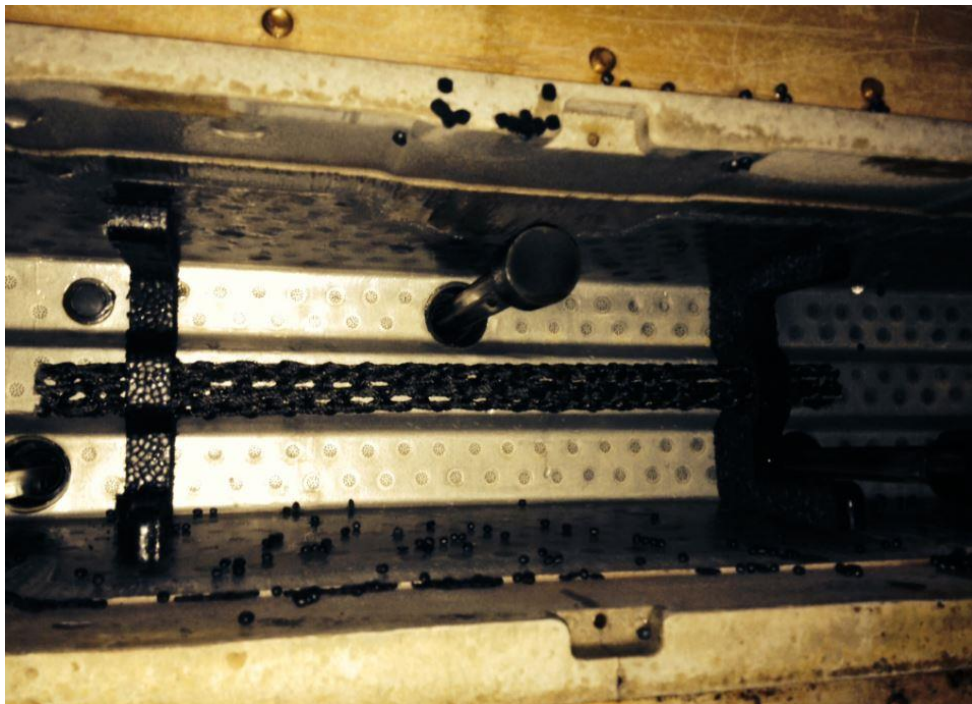


Figure 56 1 inch O-ACS held in supports placed in the mold of an EPP molding machine

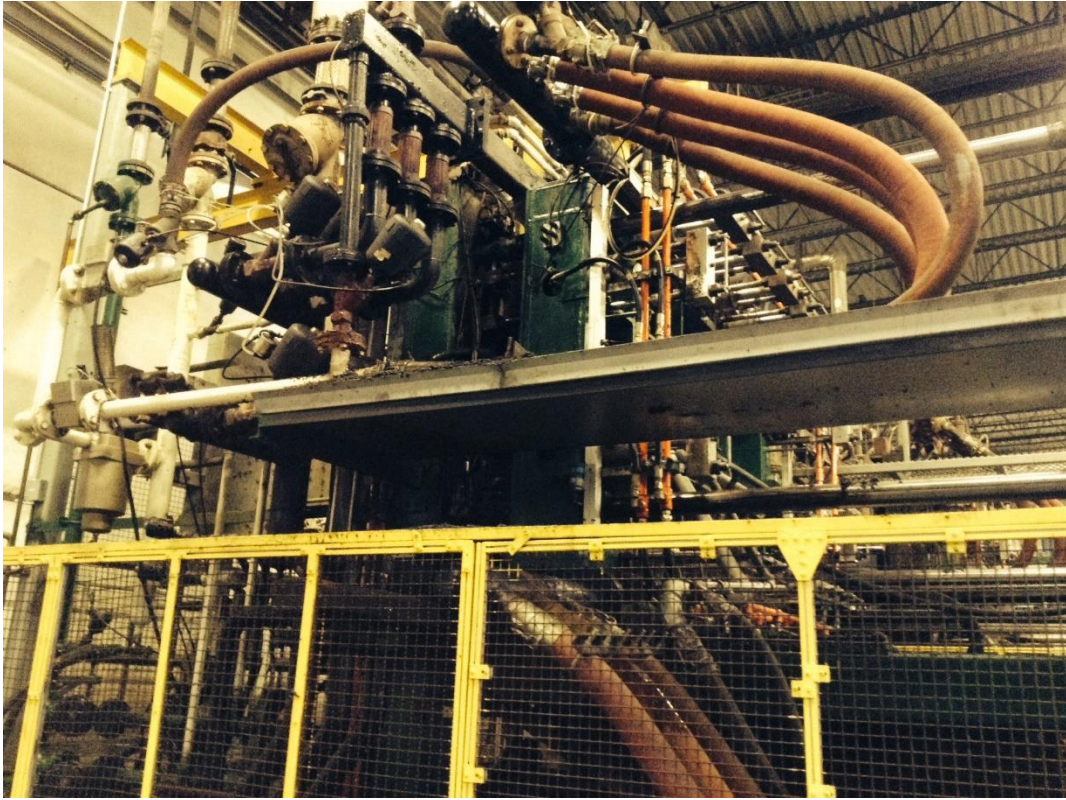


Figure 57 EPP molding machine



Figure 58 1 inch diameter O-ACS tube (1.549 gm/cm)



Figure 59 1 inch diameter O-ACS tube with EPP molded inside it (1.736 gm/cm)

Testing

The following test plan was used to conclude whether EPP helps the O-ACS tube in the intended way or not.

1. Comparative study between O-ACS with and without EPP in 3 point bending
2. Comparative study between O-ACS with and without EPP **with collars** in 3 point bending

1. Comparative study between O-ACS with and without EPP without collars in 3 point Bending.

If the EPP aids the O-ACS, in a way we expect them to, the stiffness of the tube with EPP should be higher for a given span than the stiffness of the tube with no EPP in it. Figure 60 shows the 1 inch O-ACS being tested in 3 point bending while Figure 61 shows a 1 inch O-ACS with EPP molded in it being tested in 3 point bending fixture. Due to constraints on availability of mold sizes 16:1 ratio of Length to Diameter was unable to be achieved but the length to diameter ratio was kept constant to 11:1 throughout the comparative study to remove any effect caused due to it.



Figure 60 1 inch O-ACS being tested in 3 point bending



Figure 61 1 inch O-ACS with EPP molded in it being tested in 3 point bending

The specimens were loaded at the rate 1mm/min and the force and deflection were recorded every 0.05 second. The force – deflection curves were plotted for both these tests and can be seen in the Figure 62.

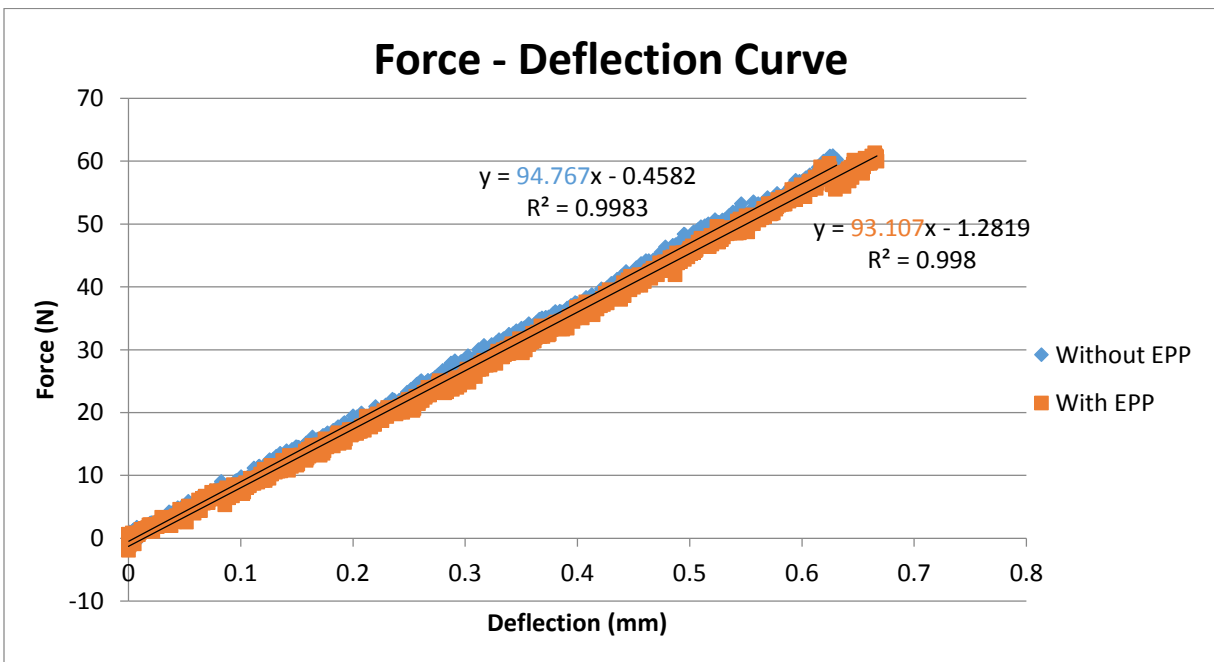


Figure 62 Force - Deflection Curves from 3 point bending test performed on O-ACS with and without EPP molded inside

As it can be seen in the figure there is not much difference in the stiffness of the tubes with and without EPP molded in it. This suggests that EPP does not have any effect on the bending stiffness of the O-ACS.

To further investigate if this is true; the O-ACS with and without EPP in it were tested on a fixed span with collars tightly fixed on them at the point of loading and also at the points of supports. Figure 63 shows a picture of the 1 inch O-ACS with collars held in the 3 point bend fixture while Figure 64 shows a picture of the 1 inch tube with EPP molded inside it with collars fixed on it for testing in the 3 point bend fixture. The length to diameter ratio was kept constant to 13:1 while testing both the specimens to remove any effect caused due to shear.

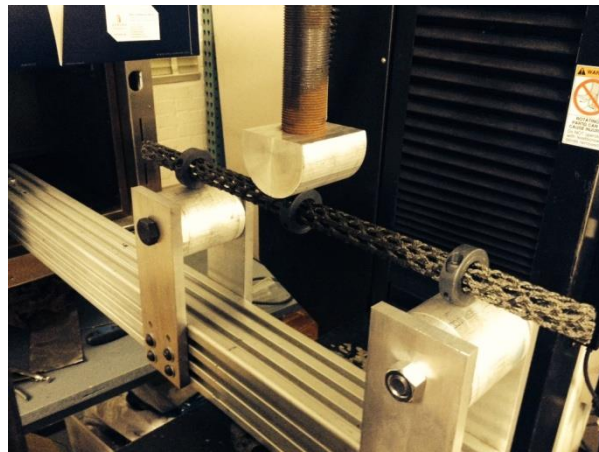


Figure 63 1 inch O-ACS being tested in modified 3 point bending



Figure 64 1 inch O-ACS with EPP molded in it being tested in modified 3 point bending

The specimens were loaded at the rate 1mm/min and the force and deflection were recorded every 0.05 seconds. The force – deflection curves were plotted for both these tests and can be seen in the Figure 65.

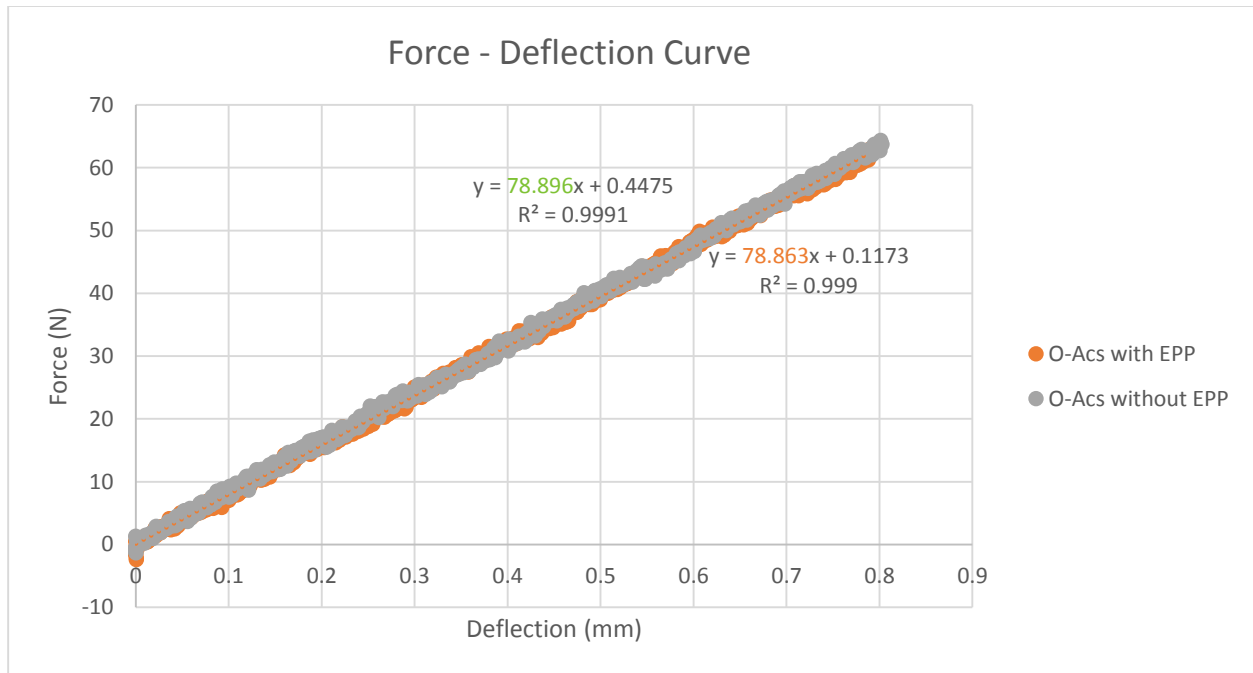


Figure 65 Force - Deflection Curves from 3 point bending test performed on O-ACS with and without EPP molded inside

The Force deflection curves of the O-ACS tested with and without EPP were almost overlapping and no considerable difference was seen in the stiffness.

Conclusion

It can therefore be safely concluded that molding EPP into the O-ACS does not help in increasing its bending stiffness. The EPP is very compliant in comparison to the structure and therefore deflects locally with the deflecting yarns under the contact loading point as well, and because of its low stiffness the EPP does not improve the overall bending stiffness of the O-ACS. As EPP is known for its energy absorbing characteristics it would be interesting to test its effect on the impact strength of the O-ACS but it is out of the scope of this study.

References

- ¹ Branscomb, D. (2012). *Minimal Weight Composites Utilizing Advanced Manufacturing Techniques*. Auburn: Auburn University.
- ² Gurley A. (2014). *Design and Analysis of Optimal Braided Composite Lattice Structures*. Auburn: Auburn University.
- ³ ASTM International. (2010). *Standard test methods for flexural properties of unreinforced and reinforced plastics and insulating materials*.
- ⁴ ASTM International. (2010). *Standard test methods for flexural properties of unreinforced and reinforced plastics and insulating materials by four point bending*.
- ⁵ ASTM International. (2014). *Standard test methods for flexural properties of fiber reinforced pultruded plastic rod*.
- ⁶ ASTM International. (2012). *Standard practice for sandwich beam flexural and shear stiffness*.
- ⁷ ASTM International. (2012). *Standard test method for facing properties of sandwich construction by long beam flexure*
- ⁸ Hibbeler, R. (2009) *Mechanics of Material*. New Jersey: Pearson Education Inc.
- ⁹ Budynas, R., Nisbett J. K. (2008). *Shigley's Mechanical Engineering Design*. New York: The McGraw-Hill Companies, Inc.
- ¹⁰ ASTM International. (2009). *Standard Test Methods of Compression Testing of Metallic Materials at Room Temperature*
- ¹¹ ASTM International. (2010). *Standard Test Methods for compressive properties of rigid plastics*
- Kothari, N. (2014). *Mechanical Characterization of the Braided Composite Yarn and Bond Strength Evaluation of the Joints of the Open-Architecture Composite Structure (O-ACS)*. Auburn: Auburn University.